

1 **Review of the Cambrian Pampean orogeny of Argentina; a**
2 **displaced orogen formerly attached to the Saldania Belt of**
3 **South Africa?**
4

5 César Casquet^{a*}, Juan A. Dahlquist^b, Sebastián O. Verdecchia^b, Edgardo G.
6 Baldo^b, Carmen Galindo^a, Carlos W. Rapela^c, Robert, J. Pankhurst^d, Matias
7 M. Morales^b, Juan A. Murra^b, C. Mark Fanning^e
8

9 *a Departamento de Petrología y Geoquímica, Facultad de Ciencias Geológicas, Instituto de*
10 *Geología Económica (CSIC), Universidad Complutense, 28040 Madrid, Spain¹*

11 *b Centro de Investigaciones en Ciencias de la Tierra (CICTERRA), CONICET, Universidad*
12 *Nacional de Córdoba, Av. Vélez Sarsfield 1611, Pab. Geol., X5016CGA Córdoba, Argentina*

13 *c Centro de Investigaciones Geológicas, CONICET, Universidad Nacional de la Plata, 1900 La*
14 *Plata, Argentina*

15 *d Visiting Research Associate, British Geological Survey, Keyworth, Nottingham NG12 5GG,*
16 *UK*

17 *e Research School of Earth Sciences, Australian National University, Canberra, ACT 0200,*
18 *Australia*
19
20

21 **Keywords:** Pampean orogeny; Saldanian orogeny; Sierras Pampeanas; Gondwana; Mara
22 terrane; collisional orogeny
23
24

25 **Abstract**
26

27 The Pampean orogeny of northern Argentina resulted from Early Cambrian oblique
28 collision of the Paleoproterozoic MARA block, formerly attached to Laurentia, with the
29 Gondwanan Kalahari and Rio de la Plata cratons. The orogen is partially preserved
30 because it is bounded by the younger Córdoba Fault on the east and by the Los Túneles
31 Ordovician shear zone on the west. In this review we correlate the Pampean Belt with
32 the Saldania orogenic belt of South Africa and argue that both formed at an active
33 continental margin fed with sediments coming mainly from the erosion of the
34 Brasiliano–Pan-African and East African–Antarctica orogens between ca. 570 and 537
35 Ma (Puncoviscana Formation) and between 557 and 552 Ma (Malmesbury Group)
36 respectively. Magmatic arcs (I-type and S-type granitoids) formed at the margin
37 between ca. 552 and 530 Ma. Further right-lateral oblique collision of MARA between
38 ca. 530 and 520 Ma produced a westward verging thickened belt. This involved an
39 upper plate with high P/T metamorphism and a lower plate with high-grade
40 intermediate to high P/T metamorphism probably resulting from crustal delamination or
41 root foundering. The Neoproterozoic to Early Cambrian sedimentary cover of MARA
42 that was part of the lower plate is only recognized in the high-grade domain along with
43 a dismembered mafic–ultramafic ophiolite probably obducted in the early stages of
44 collision. Uplift was fast in the upper plate and slower in the lower plate. Eventually the
45 Saldania and Pampean belts detached from each other along the right-lateral Córdoba
46 Fault, juxtaposing the Rio de la Plata craton against the internal high-grade zone of the

¹ Corresponding author.

E-mail address: casquet@ucm.es

47 Pampean belt.

48

49 **1. Introduction**

50

51 The Pampean Belt of central and North Western Argentina is part of a long
52 chain of Cambrian orogenic belts that formed in southwestern Gondwana. They include
53 the Araguaia belt of Brazil, the Paraguay belt of southwestern Brazil and eastern Bolivia
54 (Fig. 1), and the Saldania Belt of South Africa. The belt extends further east into the
55 Transantarctic Mountains of Antarctica and the Delamerian belt of southern Australia.
56 These belts concluded the amalgamation of Gondwana in the Early Cambrian.

57 The Pampean orogeny was first recognized in the Sierras Subandinas and the
58 Sierras Orientales of North Western Argentina (Aceñolaza and Toselli, 1973, 1976).
59 The orogeny was inferred from the Tilcarian unconformity between the allegedly Late
60 Precambrian to Early Cambrian, strongly folded, low-grade metasedimentary
61 Puncoviscana Formation and the overlaying post-orogenic middle to Late Cambrian
62 Mesón Group. This constrained its timing to Early-to-Middle Cambrian (e.g.,
63 Aceñolaza and Toselli, 1981). Further work, including precise U-Pb geochronology (for
64 a review see Baldo et al., 2014), has confirmed that the orogeny can also be recognized
65 in the easternmost Sierras Pampeanas, where there are metasedimentary rocks
66 equivalent to the Puncoviscana Formation and regional metamorphism and magmatism
67 has been dated between ca 545 and 520 Ma, i.e., Early Cambrian (Rapela et al., 1998;
68 Otamendi et al., 2004; Schwartz and Gromet, 2004; Escayola et al., 2007; Ianizzotto et
69 al., 2013; Murra et al., 2016). Cambrian magmatism has also been reported from
70 Patagonia (Hervé et al., 2010; Pankhurst et al. 2014).

71 The Pampean orogeny involved strong folding accompanied by penetrative
72 foliation, shearing and low to high-grade regional metamorphism under high P/T to
73 intermediate and low P/T conditions. The significance of this orogeny has long been a
74 matter of much debate but there is agreement now that it involved the closure of an
75 ocean to the west and concluded with the collision of continental blocks (e.g., Ramos et
76 al., 1988; Rapela et al., 1998). The main current models represent two alternative
77 tectonic interpretations: 1) orthogonal collision involving subduction beneath the Rio de
78 la Plata craton in its present relative position (Ramos et al. 2015, Fig. 10 A; and
79 references therein) or 2) transpressional orogeny that juxtaposed the orogenic belt and
80 the Rio de la Plata craton by right-lateral displacement at the end of or after the orogeny

81 (Rapela et al., 2007, 2016; Casquet et al., 2012).

82 In this contribution we present a model of the Pampean orogeny in the Sierras
83 Pampeanas and North Western Argentina particularly focused on the structural,
84 metamorphic and magmatic evolution. Correlation of the Pampean belt with the
85 Saldania Belt of southern Africa is as part of the hypothesis of significant right-lateral
86 translation (e.g., Rapela et al., 2007). The tectonic model proposed here accounts for the
87 similarities and explains the final displacement of the Pampean section of the orogenic
88 belt relative to the Saldanian orogen.

89

90 **2. Definition and Boundaries**

91

92 The Pampean belt crops out in the westernmost Sierras Pampeanas (Sierras de
93 Córdoba and Sierra Norte) and in the Cordillera Oriental of North Western Argentina.
94 The Sierras Pampeanas constitute a morphotectonic region of elongated outcrops
95 (sierras) of pre-Andean basement resulting from Cenozoic reverse faulting of the
96 Andean foreland. The width of this belt is low (ca. 100 kilometres at most) because the
97 original belt is actually truncated on both sides (Fig. 2).

98 On the eastern side is the Córdoba Fault, an important geological and
99 geophysical discontinuity that separates the Sierras Pampeanas from the Río de la Plata
100 craton (Favetto et al., 2008, Ramé & Miró, 2011; Peri et al., 2013). The latter is a
101 Paleoproterozoic block that shows no evidence of reworking by the Pampean orogeny
102 (Rapela et al., 2007): it reached its present position after right-lateral displacement
103 during and immediately after the Pampean orogeny in the Early–Middle Cambrian
104 (Rapela et al., 2007; Siegesmund et al., 2010; Drobe et al., 2009; Spagnuolo et al.,
105 2012). The Córdoba Fault has been correlated with the transcontinental Transbrasiliano
106 Lineament of Schobbenhaus Filho (1975) and Cordani et al. (2003) (Rapela et al., 2007;
107 Ramé & Miró, 2011) (Figs. 1 & 2). On its western side the Pampean orogen is
108 juxtaposed against the Ordovician Famatinian orogenic belt across the anastomosed Los
109 Tuneles–Guacha Corral ductile westward thrust (Figs. 2 & 3), which superposed the
110 internal high-grade zone of the Pampean orogen over rocks of the Conlara Complex of
111 the eastern Sierras de San Luis, probably at 440–430 Ma (Martino, 2003; Whitmeyer &
112 Simpson, 2003; Steenken et al., 2010). The Conlara Complex underwent medium-grade
113 regional metamorphism in the Early to Middle Ordovician (Steenken et al., 2006). The
114 western boundary of the Pampean orogen can be traced northward into the Sierras

115 Subandinas of North Western Argentina (Fig. 2).

116

117 **3. Metamorphic and Tectono-stratigraphic Domains.**

118

119 A primary internal division of the Pampean orogen can be made on the basis of
120 metamorphic grade. Most of the orogen consists of low-grade rocks (Fig. 2) exposed in
121 a large region embracing the Sierras Norte de Córdoba and NW Argentina together with
122 minor outcrops in the Sierra de Guasayán, Sierras de Córdoba and probably in the Sierra
123 de Ancasti (Ancasti Formation) and the eastern Sierra de San Luis (Conlara Complex).
124 In the latter cases no evidence of Pampean metamorphism has been preserved because
125 the rocks were overprinted by medium- to high-grade metamorphism during the
126 Famatinian orogeny. The second metamorphic domain corresponds for the most part to
127 the Sierras de Córdoba (Fig. 2), where Pampean metamorphism attained high-grade
128 conditions and migmatites are widespread. The boundary between these two domains
129 remains to be precisely defined. Metamorphic continuity is everywhere disrupted by
130 younger shear zones or faults such as the Carapé fault in northernmost Sierra Chica
131 (Fig. 2) which underwent significant displacement in the Ordovician (Martino, 2003).
132 However the absence of a medium-grade domain could mean that it was thinned out late
133 during the Pampean orogeny and that the overall picture was that of a mantled gneiss
134 dome (e.g., An Yin, 2004) before reworking along younger faults or shear zones.

135 The Pampean orogeny has long been considered as a case of continental
136 collisional, mainly on the evidence of metamorphic *P-T* conditions and magmatism
137 (Rapela et al., 1998; Ramos et al., 2010). Recent work on U-Pb dating of detrital zircon
138 and Sr isotope blind dating of marbles strengthens this interpretation. In fact here were
139 two contrasting sedimentary successions (see below) involved in the orogenic belt that
140 were apparently sourced from opposite continents (Casquet et al., 2012; Rapela et al.,
141 2016; Murra, 2016). This in turn implies that two main tectono-stratigraphic domains
142 exist in the Pampean orogen representing upper and lower plates. The boundary
143 between them apparently coincides with a dismembered mafic-ultramafic complex
144 whose outcrops are scattered across the Sierra Grande and Sierra Chica de Córdoba. The
145 complex consists of meta-peridotite, meta-pyroxenite, meta-gabbro, massive chromitite,
146 and minor leucocratic rocks that have been interpreted as an ophiolite (upper mantle and
147 oceanic crust), i.e., relics of a suture (e.g., Ramos et al., 2000; Escayola et al., 2007;
148 Proenza et al., 2008; Martino et al., 2010, among others).

149 The two tectono-stratigraphic domains would thus represent the two continental
150 margins that collided to produce the Pampean orogeny and the dismembered mafic-
151 ultramafic complex would be the relic of the intervening Neoproterozoic to Early
152 Cambrian oceanic lithosphere. The ocean correlates with the southern extension
153 (present coordinates) of the Clymene Ocean that existed between Amazonia and other
154 Gondwanan blocks (Trindade et al., 2006). Continental collision brought to an end the
155 amalgamation of Gondwana (Rapela et al., 2016; Murra et al., 2016).

156 The boundaries between the metamorphic domains and the Pampean suture are
157 not coincident. The upper plate is for the most part represented by the low-grade domain
158 although it was also imbricated in the high-grade domain. The lower plate however is
159 only preserved in the high-grade domain. Figure 3 shows a schematic cross-section
160 showing the hypothetical relationships between upper and lower plates. Colliding
161 blocks in Figure 3 are MARA, i.e., a Paleoproterozoic block named after three of its
162 alleged outcrops: Sierra de MAZ, Arequipa (Peru) and Rio Apa (southern Brazil)
163 according to Casquet et al. (2012) (see section 6.1) and the Kalahari - Rio de la Plata
164 cratons.

165

166 **4. The Low-Grade Domain**

167

168 *4.1 The Puncoviscana Formation*

169

170 The Puncoviscana Formation (Turner, 1960) is a thick, mainly siliciclastic,
171 partly turbiditic succession with minor limestone and volcanic beds (Ježek, 1990;
172 Omarini et al., 1999; Zimmermann, 2005; Aceñolaza and Aceñolaza, 2007) that is
173 widespread in NW Argentina. Its age and the tectonic setting of sedimentation have
174 been controversial. The term Puncoviscana Formation in the literature embraces rocks
175 stratigraphically older than the unconformably overlying Middle to late Cambrian
176 Meson Group (e.g., Omarini et al., 1999; Adams et al., 2008, 2011, and references
177 therein). Originally described as the “basal Precambrian shield” it was first recognized
178 as of Late Neoproterozoic to Early Cambrian age on the basis of trace fossils
179 (Aceñolaza and Durand, 1973; Aceñolaza and Toselli, 1976). Correlation with high-
180 grade metamorphic rocks in the eastern Sierras Pampeanas was first established by
181 Rapela et al. (1998) and confirmed by subsequent isotope studies (Schwartz and Gromet
182 2004; Rapela et al. 2007, 2016; Murra et al., 2011; Escayola, 2007, among others). This

183 thus presents the main evidence for the Early Cambrian Pampean orogeny. The
184 Puncoviscana Formation characteristically contains an almost bimodal detrital zircon
185 population with major peaks at 1100–960 Ma and 680–570 Ma and a few grains of 1.7–
186 2.0 Ga and ca. 2.6 Ga; it lacks grains derived from the nearby Rio de la Plata craton
187 (2.02–2.26 Ga) (Schwartz and Gromet, 2004; Escayola et al., 2007; Rapela et al., 2007).
188 Sedimentation took place between ca. 570 Ma and ca. 537 Ma (Rapela et al., 2007,
189 2016; Escayola et al., 2011; Aparicio González et al., 2014). Contrasting sedimentary
190 settings have been proposed, such as a passive continental margin (Do Campo &
191 Ribeiro Guevara, 2005; Piñan-Llamas & Simpson, 2006) and a shallow extensional
192 aulacogen (Aceñolaza and Toselli, 2009). A forearc basin on an active continental
193 margin resulting from oblique closure of the Clymene Ocean was suggested by Rapela
194 et al. (2007). The basin was probably not adjacent to the Rio de la Plata craton until
195 both became juxtaposed through right-lateral displacement along the Cordoba Fault
196 (Schwartz and Gromet, 2004; Rapela et al., 2007; Verdecchia et al., 2011; Casquet et
197 al., 2012). This kinematic model was accepted by Drobe et al. (2009), Siegesmund et al.
198 (2010) and Llamas & Escamilla (2013) and right-lateral displacement was found to be
199 compatible with paleomagnetic evidence (Spagnuolo et al., 2012). If *P* values of 8 - 9
200 kbar at 240° - 300° C attained during metamorphism (Do Campo et al., 2013) are
201 confirmed by future work, the Puncoviscana Formation could have originated as an
202 accretionary prism coeval with oblique eastward subduction of the Clymene Ocean.

203 Rocks with similar detrital zircon U-Pb ages are also recognized further west in
204 the Sierras de Ancasti (as the Ancasti Formation) and San Luis (Conlara Complex)
205 (Rapela et al., 2007, 2016; Steenken et al., 2006), but in both places Famatinian
206 deformation and metamorphism has overprinted the earlier structures of the
207 Puncoviscana Formation, masking the evidence for a pre-Famatinian event (Steenken et
208 al., 2006). Verdecchia et al. (2012) showed that medium-grade metamorphism of the
209 Ancasti Formation resulted from a single event of Famatinian age, so that this and the
210 Conlara Complex were probably originally akin to the low-grade Puncoviscana
211 Formation elsewhere.

212 A large outcrop of phyllite equivalent to the Puncoviscana Formation is found
213 near Los Tuneles (the Los Túneles Phyllites of Rapela et al., 1998; Escayola et al.,
214 2007) (Figs. 2 & 3) (Baldo et al., 1996; Rapela et al., 1998; Escayola et al., 2007),
215 where it is separated by faults and shear zones from the high-grade domain (Martino et
216 al., 2003).

217 One sample from the Los Túneles Phyllites (TLT-2069) has been analysed for
218 U-Pb SHRIMP zircon chronology and $\delta^{18}\text{O}$ and Hf isotope measurements on dated
219 zircon (analytical methods as in Rapela et al., 2016) for comparison with North Western
220 Argentina and the Saldania Belt (see Discussion section). The results from TLT-2069
221 are shown in Tables 1 and 2, and detrital zircon ages represented in Fig. 4. This age
222 spectrum shows two well defined peaks in the ranges 562–690 Ma and 953–1100 Ma
223 typical of the Puncoviscana Formation (Rapela et al., 2016). There are a few single
224 grains ages of 777, 890, 1240 1880 and 2505 Ma. The $\delta^{18}\text{O}$ values range from +5.74‰
225 to +10.71‰. The εHf_t values are positive (+0.7 to +12.0) and Hf model ages (single-
226 stage) are in the range 710 –1440 Ma.

227

228 *4.2 The magmatic arc*

229

230 The mostly low-grade upper plate domain comprises low-grade clastic
231 metasedimentary rocks equivalent to the monotonous Late Neoproterozoic to Early
232 Cambrian Puncoviscana Formation. It hosts a Cordilleran calc-alkaline magmatic arc of
233 Early Cambrian age – the Sierra Norte–Ambargasta batholith, the Tastil and other
234 plutons in NW Argentina. The arc rocks are I-type metaluminous to slightly
235 peraluminous, ranging from diorite to leucogranite, dacite porphyry and even volcanic
236 rocks (rhyolite) and tuffs. U-Pb zircon ages of plutons, dykes and tuffs that can be
237 confidently attributed to the Pampean orogeny range from 541 ± 4 to 523 ± 2 Ma
238 (Lyons et al., 1997; Rapela et al., 1998; Stuart-Smith et al., 1999; Leal et al., 2003;
239 Hauser et al., 2011; Escayola et al., 2007, 2011; Tibaldi et al., 2008; Aparicio Gonzalez
240 et al., 2011; Hong et al., 2010; Siegesmund et al., 2010; Iannizzotto et al., 2013; von
241 Gosen et al., 2014; Dahlquist et al., 2016) (Table 3). The metaluminous Sierra Norte–
242 Ambargasta batholith was emplaced within a very short period of time: the main
243 intrusive pulse took place between 537 ± 4 and 528 ± 2 Ma (based on 11 results) with
244 most ages in the range 530 ± 4 Ma (Rapela et al., 1998; Leal et al., 2003; Siegesmund et
245 al., 2010; Iannizzotto et al., 2013; von Gosen et al., 2014; Table 3) and thus constitutes
246 a magmatic flare-up. This pulse was largely coeval with regional compressional strain
247 (Iannizzotto et al., 2013; Von Gosen et al., 2014). Volcanic rocks of 531 ± 4 Ma (Agua
248 del Rio dacite porphyry) (Table 3) and 531 ± 3 Ma (Rodeito rhyolite-dacite; age
249 recalculated from $^{206}\text{Pb}/^{238}\text{U}$ ages after Von Gosen et al., 2014) attest to their
250 contemporaneity with plutonism.

251 A group of rhyolites and granites with ages between 519 ± 4 and 512 ± 4 Ma
252 (Table 3) is probably related to late orogenic uplift (Ramos et al., 2015). However,
253 younger ages should be viewed with care because of Pb-loss since the Pampean realm
254 (both upper and lower plates) underwent significant reheating during the Famatinian
255 orogeny (490–440 Ma) (Rapela et al., 1998). In any case, ages younger than ca. 520 Ma
256 quoted by other authors (see Table 3) are taken here as resulting from post-Pampean
257 orogeny processes.

258 Hf isotope composition of zircon (Table 3) is so far only available for the Tastil
259 pluton, a dacitic porphyry in NW Argentina (Hauser et al., 2011) and the small granite
260 body of Guasayán pluton (533 ± 4 Ma, Dahlquist et al., 2016) (Fig. 2). The $\epsilon_{\text{Hf}t}$ values
261 range from +1.1 to -6.9 and the Hf T_{DM} model ages are in the range 1.3 to 1.7 Ga. Nd-
262 isotope compositions are available for the Sierra Grande–Ambargasta batholith and for
263 NW Argentina (Hauser et al., 2011; Iannizzotto et al., 2013) (Table 3): $\epsilon_{\text{Nd}t}$ values
264 range between ca. -2 and -10 and the Nd T_{DM} model ages 1.4 to 2.0 Ga. The Nd model
265 ages of the Puncoviscana Formation represent the crustal age of the upper plate,
266 ranging from ca. 1.7 to 2.0 Ga (most are ca. 1.7 Ga) (Bock et al., 2000; Lucassen et al.,
267 2000; Rapela et al., 1998). This range of Nd model ages is compatible with that found
268 for the Pampean magmatic arc (1.5 – 2.0 Ga), perhaps with the additional effect of a
269 minor juvenile component.

270

271 *4.3 Structural features and metamorphic conditions in the upper plate*

272

273 Strain in the upper plate was distributed between sub-domains with upright to
274 west-vergent folds with axial-planar foliation and dextral NE–SW trending mylonite
275 corridors such as the large Sauce Punco shear zone in Sierra Norte (Martino, 1999; von
276 Gosen and Prozzi, 2010). Magma emplacement was largely focused along shear zones
277 and plutons are both earlier and later with respect to shearing (e.g., Iannizzotto et al.,
278 2013). This domain continues in North Western Argentina where metasedimentary
279 rocks of the Puncoviscana Formation are abundant. Metamorphism here was very low-
280 grade to low-grade and was coeval with folding and shearing (von Gosen & Prozzi,
281 2010). P - T conditions for $M1_{\text{up}}$ (up indicating upper plate) were recently rated at 8 – 9
282 kbar and 240 – 300°C, i.e., a high P/T type of metamorphism (Do Campo et al., 2013);
283 this was followed by isothermal decompression through 275 – 350 °C and 0.7 – 3.0 kbar
284 ($M2_{\text{up}}$) (Table 4 ; Fig. 5). Rapid uplift and erosion resulted in volcanism with ages

285 indistinguishable within error from those of the underlying plutonic rocks (see below).

286 In the northern Sierras Pampeanas a discordant fanning foliation (S_{1up}) is
287 associated with ubiquitous metric/decametric-scale chevron folds that have subvertical
288 axial planes. These structures resulted from a single major deformation episode (Piñán-
289 Llamas & Simpson, 2006). Tectonic foliation overprints pressure-solution cleavage and
290 banding is interpreted as a compaction-related primary foliation (Piñán-Llamas &
291 Simpson, 2009).

292 Outcrops of low-grade Puncoviscana Formation are also found to the west of the
293 high-grade domain as isolated lenses separated from the latter domain by shear zones
294 and faults. Such is the case of the Los Túneles Phyllites in the westernmost Sierra
295 Grande de Córdoba (Martino et al., 2003; Escayola et al., 2007). The phyllites
296 underwent Pampean metamorphism at 525 ± 18 Ma (whole rock Rb-Sr isochron,
297 MSWD = 25; Rapela et al., 1998).

298

299 **5. The High-Grade Domain**

300

301 *5.1 The Sierras de Córdoba Metasedimentary Series*

302

303 This domain consists for the most part of high-grade metasedimentary migmatitic
304 gneisses of the Puncoviscana Formation and migmatite gneisses, marbles and calc-
305 silicate rocks that were recently included within the Sierras de Córdoba
306 Metasedimentary Series by Murra et al. (2016). Late Ediacaran to Early Cambrian ages
307 were indirectly determined for the latter from the Sr-isotope composition of chemically
308 screened samples of almost pure calcite marble and were further constrained by C- and
309 O-isotope data and U-Pb SHRIMP detrital zircon ages of an interbedded paragneiss
310 (Murra et al., 2016). The marbles show two groups of $^{87}\text{Sr}/^{86}\text{Sr}$ ratios (ca. 0.7075 and
311 0.7085), inferred as corresponding to Early Ediacaran (620 to 635 Ma) and Late
312 Ediacaran to Early Cambrian, respectively. Interbedded migmatitic gneisses have
313 detrital zircon age patterns that show a group of ages between ca. 700 and 1650 Ma;
314 there is a notable peak at ca. 1190 Ma (range 1100–1250 Ma), and an older population
315 with ages of ca. 1950 – 2060 Ma (in contrast, the Puncoviscana Formation lacks ages
316 between ca. 1.2 and 1.65 Ga but has a characteristic Neoproterozoic peak between 570
317 and 680 Ma that is missing here). The Sierras de Córdoba Metasedimentary Series
318 pattern instead resembles those of rocks from the Western Sierras Pampeanas, such as

319 the Difunta Correa Sedimentary Sequence and the Ancajan Series, which are also
320 interbedded with Ediacaran marbles (Ramacciotti et al., 2015; Rapela et al., 2016). This
321 correlation implies that all belong to an originally extensive sedimentary cover to
322 Mesoproterozoic (Grenvillian *s.l.*) basement (Murra et al., 2016). The source of these
323 metasedimentary series has been ascribed to the Mesoproterozoic (and
324 Paleoproterozoic) basement of the Western Sierras Pampeanas and further west
325 (Laurentia?) (Ramacciotti et al., 2015; Rapela et al., 2016). In contrast, the Late
326 Ediacaran to Early Cambrian Puncoviscana Formation of NW Argentina, northern
327 Sierra Chica and Sierra Norte, is thought to have had sedimentary input from Gondwana
328 continental sources (Murra et al., 2016).

329

330 5.2 *The ophiolite*

331

332 The mafic–ultramafic complex consists of meta-peridotite, meta-pyroxenite
333 meta-gabbro, massive chromitite, and minor leucocratic rocks that were collectively
334 interpreted as an ophiolite complex (upper mantle and oceanic crust) and hence a relict
335 suture (e.g., Ramos et al., 2000, Escayola et al., 2007, Proenza et al., 2008, Martino et
336 al., 2010, among other). The ophiolite probably formed in a supra-subduction setting on
337 the basis of basalt chemistry that ranges from N-MORB to OIB; it has yielded a Sm-Nd
338 age of 647 ± 77 Ma (Escayola et al., 2007). Ophiolite remnants are found in the inner
339 part of the Pampean orogenic wedge now exposed in the Sierras de Cordoba. They
340 underwent Pampean high-grade metamorphism and deformation (e.g., Martino et al.,
341 2010; Tibaldi et al., 2008) that overprinted the obduction-related structures that
342 preceded continental collision. Remarkably the ophiolite outcrops are often spatially
343 associated with marbles, calc-silicate rocks and gneisses of the Sierras de Cordoba
344 Metasedimentary Series (Fig. 1, Kraemer et al., 1995; Martino, 2003), strengthening the
345 idea that the ophiolite was obducted onto the carbonate platform at the western margin
346 of the Clymene Ocean in a similar manner to the Oman ophiolite (Escayola et al.,
347 2007). The ophiolite was then involved in the Pampean orogenic wedge and imbricated
348 with slivers of rocks of the upper plate (Puncoviscana Formation).

349 N-MORB type tholeiitic amphibolites are also found as disrupted bodies closely
350 associated with the Sierras de Cordoba Metasedimentary Series (Rapela et al., 1998).
351 The age and significance of these rocks, whether related to the ophiolite or to early
352 processes along the active margin remain unknown.

353

354 *5.3 Structural Geology*

355

356 The large scale structural geology of the high-grade Pampean domain is poorly
357 known. Early work by Martino et al. (1995) and Baldo et al. (1996) recognized a
358 regional shallow-dipping axial planar foliation (S2) related to west-verging isoclinal
359 folds (D2) and coeval with high-grade intermediate *P/T* metamorphism (M1) which
360 peaked at 530–520 Ma (Rapela et al., 1998; Murra et al., 2016). After allowing for
361 block tilting during Cenozoic compression, the regional foliation is almost flat-lying.
362 An older foliation is locally preserved in rafts in migmatitic granitoids and is interpreted
363 as an S1 foliation re-folded and transposed by S2. Continued deformation led to
364 shearing along discrete zones (D3 according to Martino et al. (2010). D2 folding and D3
365 shearing was accompanied by crustal thickening, with recorded *P* values of up to 7–9
366 kbar under upper amphibolite to granulite facies conditions (see below; Rapela et al.,
367 1998; Otamendi et al., 1999; Martino et al., 2010). Mafic and ultramafic bodies are
368 often aligned with bands of marble, calc-silicate hornfelses and gneisses of the Sierra de
369 Córdoba Metasedimentary Series, and with the S2 foliation. They were formerly
370 considered to define two regional strips (e.g., Kramer et al., 1995) but this interpretation
371 has been recently challenged, i.e., mafic–ultramafic bodies are repeated by folding and
372 shearing and there is no regular regional pattern (Fig. 3) (Martino et al., 2010). These
373 bodies underwent M2 metamorphism (see below) (Rapela et al., 1998; Tibaldi et al.,
374 2008; Anzil et al., 2012). The high-grade domain further underwent uplift at ca. 525–
375 520 Ma, accompanied by strongly peraluminous magmatism such as the El Pílon
376 cordierite (see below). The latter complex resulted from magma displacement from ca.
377 6 to 3.7 kbar at 523 ± 2 Ma (Rapela et al., 1998, 2002) favoured by regional
378 decompression, probably during mantled-gneiss dome formation. Structures related to
379 uplift of the Pampean orogen are as yet poorly known: one example is the eastern side
380 of the large Guacha Corral shear zone in the Santa Rosa area, where dextral movement
381 combined with extension in narrow mylonitic belts was recorded by Martino et al.
382 (1994; Fig.5).

383 Foliation S2 in the lower plate may be correlated with the S1 foliation dominant
384 in the low-grade domain of the upper plate. However the thermal peak may have been
385 attained later in the high-grade domain (527 ± 3 Ma) than in the low-grade upper plate
386 domain (530 ± 4 Ma; minimum age).

387

388 *5.4 Regional metamorphism and anatectic magmatism*

389

390 Metamorphism in the Pampean orogen high-grade domain has been the subject
391 of work by many authors (Table 4). Most have focused on metapelitic gneisses and
392 migmatites and a few on mafic granulites (metabasites) (Table 4). Migmatites are
393 represented by metatexites and diatexites mostly consisting of garnet–biotite–
394 plagioclase–quartz–K feldspar \pm sillimanite \pm cordierite (see Guerreschi and Martino,
395 2014). The metabasites consist of plagioclase–orthopyroxene–biotite–quartz–garnet–
396 amphibole (e.g., Rapela et al., 1998; Otamendi et al., 2005). There is some evidence of
397 an older M1_{lp} metamorphic event (lp = lower plate) in the form of aligned inclusions in
398 garnet, but its *P-T* conditions are unknown. M2_{lp} corresponds to the high-grade event
399 under granulite-facies conditions. Garnet \pm cordierite migmatites from central to
400 northern and eastern Sierras de Córdoba yield *P-T* estimates (conventional
401 thermobarometry) of 750–850 °C for peak *T* and 7–8 kbar for the maximum recorded *P*
402 (Fig. 5) (Baldo et al., 1996; Rapela et al., 1998; Otamendi et al., 1999, 2005). However
403 N–S longitudinal *P-T* gradients probably existed.

404 The ages obtained for the peak of metamorphism are apparently younger than
405 those in the low-grade domain, between 530 and 520 Ma (Lyons et al., 1997; Rapela et
406 al., 1998 among others). A recent U-Pb SHRIMP zircon age of 527 \pm 3 Ma was
407 reported by Murra et al. (2016). The high *P* values for the high-grade granulite-facies
408 domain suggest that underthrusting played a role and that an orogenic root probably
409 formed within a few million years.

410 Metamorphism-related S-type peraluminous magmatism (Table 3) is represented
411 by several granitic complexes such as El Pilón (ASI = 1.08–1.40) dated at 523 \pm 2 Ma
412 (conventional U-Pb, Rapela et al., 1998, 2000), the San Carlos migmatitic massif (529 \pm
413 3 Ma; Escayola et al., 2007), Suya Taco (520 \pm 3 Ma, U-Pb on monazite, Tibaldi et al.,
414 2008). These ages suggest that peraluminous magmatism took place after the I-type
415 magmatism and was related to the high-grade M2_{lp} event. Nd-isotope data from the El
416 Pilón and San Carlos complexes yielded consistent values of ϵ Nd_t of ca. -5.7 and Nd
417 model ages (T_{DM}) of 1.6–1.7 Ga, compatible with derivation by melting of fertile
418 supracrustal rocks.

419 The conditions of retrograde metamorphism are poorly constrained (Table 4;
420 Fig. 5). After intrusion at a depth of ca. 6 kbar (and ca. 780°C), the El Pilón granitic

421 complex re-equilibrated with the host migmatites at $T = 555 \pm 50^\circ\text{C}$ and $P = 3.3 \pm 0.3$
422 kbar (Rapela et al., 2002). These values imply a gross uplift rate of ca. 2.4 mm/a
423 accompanied by cooling of 280 – 180°C subject to analytical errors. In Fig. 5, an
424 estimate uplift P - T path has been drawn based on data from several sources.

425 Evidence of thermal events older than M2_{lp} is contentious. Metamorphism
426 related to early ridge subduction was invoked by Simpson et al. (2003), Gromet et al.
427 (2005) and Guerreschi & Martino (2008) to explain the high temperatures attained in the
428 high-grade domain but this mechanism is not supported by the P values of up to 8 kbar
429 referred to above and chronological constraints – in fact the peak of metamorphism
430 (M2) is younger than the magmatic arc in the Pampean belt. Siegesmund et al. (2010)
431 showed that some high-grade gneisses and diatexites from the Eastern Sierras
432 Pampeanas contain zircon grains with low U/Th overgrowths interpreted as of
433 metamorphic origin and dated at ca. 550–540 Ma. If confirmed by further research this
434 cryptic metamorphism could correspond to the early (phase I) S-type granitic
435 magmatism in the Saldania Belt (see below).

436

437 **6. Discussion**

438

439 *6.1 The geodynamic framework*

440

441 Current models on the evolution of the Pampean belt fall into one of two types.
442 According to Escayola et al. (2007) and Ramos et al. (2014) an ocean existed on the
443 eastern side of a Grenvillian terrane called Pampia before 0.7 Ga. The Puncoviscana
444 Formation began to form on this margin, receiving zircon from the west with ages
445 between 1.0 and 1.2 Ga. Subsequent intra-oceanic west-directed subduction started at
446 700–600 Ma, with development of a magmatic island-arc and a back-arc region between
447 this and Pampia. The arc supplied zircon of 0.6–0.7 Ga to the adjacent continental
448 margin thus explaining, according to these authors, the typical Puncoviscana detrital
449 zircon pattern. A consequence of this model is that the Puncoviscana Formation formed
450 in part after 1.1 Ga and before 700 Ma, and in part during and after the island arc
451 activity when zircon from Pampia and the arc mingled in the sediment. However no
452 sedimentary rocks have ever been found from the Puncoviscana Formation, i.e. with the
453 characteristic detrital zircon age peak between 950 and 1100 Ma (Rapela et al., 2016),
454 as old as Tonian (> ca. 720 Ma), nor have rocks been found with a single peak of 0.6–

455 0.7 Ga, as might be expected close to the island arc source area. All the evidence from
456 detrital zircon ages and paleontology (see above) suggest that the Puncoviscana
457 Formation is younger than 570 Ma and that the sources were in the east. Moreover most
458 zircon from the Puncoviscana Formation between 560 and 700 Ma have negative ϵ_{Hf_t}
459 values suggesting a continental provenance. The next step in this type of model is
460 obduction of the island arc over the Rio de la Plata craton at 600–580 Ma, accompanied
461 by a flip of the subduction zone from west-dipping to east-dipping, for which there is no
462 direct evidence. The Rio de la Plata craton was not affected by the Pampean orogeny.
463 Collision between Pampia and the Rio de la Plata craton took place between 580–540
464 Ma and was followed by decompression melting and metamorphism between 540 and
465 515 Ma. However the thickening-related M2 metamorphism in the high-grade zone that
466 yielded P values of up to ca. 8 kbar took between 530 and 525 Ma (see above).
467 Furthermore no account is taken in this model of sedimentary rocks such as the late
468 Neoproterozoic Sierras de Córdoba Metasedimentary Series of age (Murra et al., 2016),
469 for which Grenville-age (0.95–1.45 Ga) zircon was sourced from the Western Sierras
470 Pampeanas basement and yet further west from Laurentia (Rapela et al., 2016).

471 In another view the collisional Pampean orogeny resulted from the closure of
472 the intervening Clymene Ocean hypothesized on the basis of paleomagnetic evidence as
473 located between Amazonia and Laurentia on one side and West Gondwana cratons such
474 as Rio de la Plata and Kalahari on the other (Trindade et al., 2006; Rapela et al., 2007).
475 Colliding blocks were considered either para-autochthonous to the Gondwana margin
476 (Rapela et al., 1998; Ramos et al., 1988, 2010) or allochthonous (Rapela et al., 2007).
477 The latter case invokes a Paleoproterozoic block formerly attached to Laurentia and
478 Amazonia during Mesoproterozoic (Grenvillian *s.l.*) continental collisions. This block
479 was named MARA after three of its alleged outcrops: Sierra de **MAZ** in the Western
480 Sierras Pampeanas, **Arequipa** (Peru) and **Rio Apa** (southern Brazil) (Casquet et al.,
481 2012). This block along with Amazonia rifted away from Laurentia during the Early
482 Cambrian opening of the Iapetus Ocean (Dalziel, 1997; Casquet et al., 2012; Rapela et
483 al., 2016). At the same time oblique right-lateral subduction of the Clymene Ocean
484 started under the West Gondwana cratons, ending with right-lateral collision of
485 MARA+Amazonia and consequent development of the Pampean, Paraguay and
486 Araguaia collisional belts (Fig. 1) (Casquet et al., 2012; Rapela et al., 2016). In this
487 model the mainly turbiditic sediments of the Puncoviscana Formation were derived
488 from Gondwana sources in the east (in the present-day sense) while the Sierras de

489 Córdoba Metasedimentary Series was sourced from the west, i.e. from the MARA block
490 and from Laurentia prior to break-up. Evidence for this interpretation is consistent with
491 the U-Pb detrital zircon evidence (see above) and the Early Ediacaran and Late
492 Ediacaran to Early Cambrian age of marbles (Murra et al., 2016). In this model the
493 Pampean orogen was displaced right-laterally during subduction and collision and
494 attained its present position relative to the Rio de la Plata craton after orogenic uplift.

495

496 *6.2 Comparison of the Pampean Belt with the Saldanian Belt of South Africa*

497

498 The Saldania Belt of South Africa consists of scattered outcrops and inliers of
499 Ediacaran to Early Cambrian low-grade metasedimentary rocks and Cambrian
500 granitoids (the Cape Granite Suite): these are unconformably overlain by Gondwanan
501 Permo-Triassic sedimentary rocks of the Cape Fold Belt. The Saldanian orogeny took
502 place in the Early Cambrian (pre-520 Ma) (Rozendaal et al., 1999; Curtis, 2001;
503 Chemale et al., 2011). The metasedimentary rocks are partly a para-autochthonous
504 cover to the Late Mesoproterozoic (Grenvillian) Natal–Namaqua basement in the
505 northeast (i.e., the Boland Group), but most have been assigned to the Malmesbury
506 Group (the allochthonous Malmesbury Terrane) which has unknown relationships to the
507 basement (Rozendaal et al., 1999; Frimmel et al., 2013).

508 The Malmesbury Group turbidites (and the Kangoo Caves Group in eastern
509 inliers, Naidoo et al., 2013) bear a strong resemblance to the Puncoviscana Formation of
510 Argentina. In particular the detrital U-Pb zircon age pattern shows many similarities.
511 Armstrong et al. (1998) found in one turbidite a bimodal distribution of ages peaking at
512 900–1050 Ma and 575–700 Ma, with a youngest zircon of 560 Ma. Frimmel et al.
513 (2013) analyzed several rocks (one argillite and three greywackes) from the
514 Malmesbury Group. The youngest concordant zircon had ages of 550–600 Ma in three
515 cases, and sedimentation age was constrained to between 557 and 552 Ma (Late
516 Ediacaran). Most grains are Neoproterozoic with many minor peaks. One main group of
517 ages can be recognized as ca. 580–700 Ma and a second group as 700–960 Ma.
518 Grenville-age detrital grains constitute a smaller group between 960 and 1100 Ma. Very
519 few grains of ca. 1.2, 1.3, 2.1 and 2.0 Ga and few Archean grains of ca. 2.7 Ga were
520 also found (Fig. 4). As noted above, the U-Pb zircon age pattern of the Puncoviscana
521 Formation is bimodal with major peaks at 1100–960 Ma and 680–570 Ma and few
522 grains of 1.7–2.0 Ga and ca. 2.6 Ga (Rapela et al., 2007, 2016; Adams et al., 2008;

523 Hauser et al., 2011). In Fig. 4, we compare the zircon age pattern from the Tygerberg
524 Formation of the Malmesbury Group (HFS08-06; Frimmel et al., 2013) with the
525 Puncoviscana sample TLT-2069. Both age patterns have the same two main groups –
526 one between 560 and 690 Ma and a Grenvillian group between 960 and 1100 Ma. A
527 small group of grains between 700 and 900 Ma in the Malmesbury sample is poorly
528 represented in the Puncoviscana sample (two grains only of 777 and 890 Ma), but is
529 more significant in other Puncoviscana samples (e.g. sample RCX-1; Adams et al.,
530 2008). The few Mesoproterozoic ages (1.2 Ga in TLT-2069 and 1.3–1.35 Ga in the
531 Tygerberg Formation) are not coincident, although the 1.2 Ga peak is recognized in
532 other samples from the Malmesbury Group. Significantly, the Puncoviscana Formation
533 and the Malmesbury Group share one important feature feature, i.e., the absence of
534 zircon with the Rio de la Plata craton ages between 2.02 and 2.26 Ga (Rapela et al.,
535 2007).

536 The comparison can be extended to the Hf composition of detrital zircon (Fig.
537 6). We have chosen the time interval 570–680 Ma, corresponding to the Brasiliano–
538 Pan-African orogeny, for this comparison, using data from North Western Argentina
539 (Hauser et al., 2011; Augustsson et al., 2016) and sample TLT-2069 (Table 2) along
540 with data from the Saldania Belt (Frimmel et al., 2013). The ϵHf_t values of the latter
541 (+4.7 to -19.2) are for the most part negative and coincident with those of the
542 Puncoviscana Formation (+ 5.8 to -18.4), suggesting Brasiliano–Pan African sources for
543 both (Frimmel et al., 2013). However sample TLT-2069 yields mainly positive ϵHf_t
544 values between + 0.7 and +12.0 and the source of these zircon grains must be different,
545 perhaps in the Neoproterozoic East African–Antarctic orogen (EAAO) as formerly
546 suggested by Rapela et al. (2007, 2016). In Fig. 6, zircon within the chosen age range
547 from the Mecuburí Formation of NE Mozambique (Thomas et al., 2010) yielded mostly
548 positive ϵHf_t values in the range +9.9 to -3.8 similar to those of sample TLT-2069. The
549 EAAO was in fact a major source of molasse sediments to the southern Kalahari
550 continental margin in Late Neoproterozoic–Early Paleozoic times (Jacobs & Thomas,
551 2004).

552 We conclude that the Puncoviscana Formation embraces Ediacaran turbidite
553 sediments derived from different continental sources with a detrital zircon age pattern
554 resembling that of the Malmesbury Group of the Saldania Belt. This pattern is in fact
555 typical of southern Gondwanan sources in general (Kristoffersen et al., 2016). One

556 source probably was in the Brasiliano–Pan-African orogenic belt that resulted from the
557 closure of the Adamastor Ocean (Frimmel et al., 2013; Rapela et al., 2011) and
558 references therein); another source probably was in the EAAO (Rapela et al., 2007,
559 2016).

560 Moreover, tectonic structure of the Pampean Puncoviscana Formation and the
561 Saldanian Malmesbury Group are very similar. Both are simple consisting of essentially
562 upright folds with axial planar foliation (Piñan-Llamas & Simpson, 2006; Rozeendal et
563 al. 1994; Buggisch et al., 2010; Rowe et al., 2010).

564

565

566 *6.3 The Cape Granite Suite and the Pampean magmatic arc*

567

568 The Pan-African Cape Granite Suite (CGS) is predominantly composed of 552
569 to 533 Ma S- and I-type granitoids that formed during the Saldanian orogeny (Table 3).
570 Scheepers (1995, and references therein) and da Silva et al. (2000) divided the orogenic
571 magmatism into two main episodes: phase I, S-type (ASI = 0.98 to 1.66) synorogenic
572 granites, and phase II, late-orogenic calc-alkaline I-type (ASI = 0.86 to 1.08) granites.
573 Phase I is bracketed between 552 ± 4 Ma and 533 ± 2 Ma (with many ages close to 540
574 Ma), and Phase 2 is dated at 536 ± 5 Ma (da Silva et al., 2000; Scheepers and
575 Armstrong, 2002; Chemale et al., 2011; Villaros et al., 2012). Minor post-orogenic S-
576 type granites and volcanics and A-type plutonic bodies intruded granites of both phases
577 as well as the Malmesbury Group metasediments between 527 ± 8 Ma and 510 ± 4 Ma
578 (Scheepers and Armstrong, 2002; Chemale et al., 2011). The post-orogenic S-type
579 granites (ca. 527 Ma) may have been emplaced in a different geodynamic setting to that
580 invoked for Phase I. The youngest peraluminous magmatism was the extrusion of S-
581 type ignimbrites at 516 ± 3 Ma (Scheepers and Poujol 2002). A-type post-orogenic
582 granitoids and the late ignimbrites will not be dealt with further here. Phase I S-type
583 granites occur inward, in the Tygerberg terrane and are usually deformed; Phase II I-
584 type granites occur outward, i.e., towards the craton, and are generally undeformed
585 (Chemale et al., 2011).

586 Nd- and Hf isotope data from the Cape Granite Suite have been reported by
587 Chemale et al. (2011) (Table 3 & 5). The ϵNd_t values of S-type granitoids (at ca.
588 550Ma) range from -3.2 to -4.9 and the Nd model ages (T_{DM}) from 1.5 to 1.9 Ga. Late
589 peraluminous granitoids yield ϵNd_t values of -5.9 and $T_{\text{DM}} = 1.7$ Ga. The ϵNd_t values of

590 high K-calc-alkaline I-type granitoids range from -1.4 to -3.9 and the T_{DM} ages from 1.0
591 to 2.0 Ga . The ϵNd_t values of the I-type granitoids are in general higher than for the S-
592 type granites suggesting a larger juvenile component in magma evolution (Chemale et
593 al., 2011). Hf isotope compositions of zircon have been reported from S-type granites of
594 the Cape Granite Suite by Villaros et al. (2012) and Farina et al. (2014) (Table 3).
595 Magmatic zircon and magmatic overgrowths show a restricted range of ϵHf_t between -
596 8.6 and +1.5 (Villaros et al., 2012), interpreted as indicating that the granitic magma
597 resulted from the anatexis of Malmesbury Group metasedimentary rocks, thus
598 confirming the S-type signature of these granites.

599 A comparison between the I- and S-type Cape Granite suite and the Pampean
600 magmatic arc rocks is shown in Table 5. I-type magmatism was roughly coeval in the
601 two belts with most ages mainly between 535 and 525 Ma and post-orogenic
602 peraluminous S-type granites of ca 527–524 Ma in the Cape Granite suite (Chemale et
603 al., 2011) are coeval with those of the high-grade domain in the Sierras de Córdoba
604 (e.g., ca. 523 Ma; Rapela et al., 1998). Nd- and Hf isotope data of I-type granitoids are
605 slightly more juvenile in the Cape Granite Suite than in the Sierras Pampeanas and NW
606 Argentina.

607 Phase I S-type granites between ca. 552 and 533 Ma (most values ca. 540Ma)
608 represent an earlier event in the Saldania Belt. Anatexis of Malmesbury Group
609 sediments apparently involved fast heating (ca. 30°/Ma) to ca. 850°C because of the
610 short time span between the youngest detrital zircon and the age of magmatism (Farina
611 et al., 2014). This older event apparently preceded the formation of the I-type
612 Cordilleran magmatic arc and has not been recognized in Argentina; although
613 Siegesmund et al. (2010) interpreted that some high-grade gneisses and diatexites in the
614 Eastern Sierras Pampeanas record a metamorphism at ca. 550-540 Ma. The significance
615 of an early, high-T metamorphism and related S-type magmatism (in the Saldania Belt,
616 at least) remains unknown. In this regard, both the hypothesis of a ridge-subduction
617 stage proposed by Gromet & Simpson (2003) for the Pampean orogeny and of an
618 extension of the accretionary prism previous to continental collision remain potential
619 options.

620

621 **7. A paleogeographic and dynamic model**

622

623 The Pampean orogeny took place between ca. 545 (and may be as old as 550Ma)

624 and 520 Ma and involved early subduction of the Clymene Ocean, development of a
625 magmatic arc and final continental collision with preservation of a suture recognized in
626 the Sierras de Córdoba. The similarities shown here between the sedimentary rocks of
627 the Malmesbury Terrane (Frimmel et al., 2013) and those of the Puncoviscana
628 Formation strengthens the hypothesis already suggested by others that both formations
629 were laid down in the same sedimentary basin probably along the southern margin of
630 the Kalahari craton (Fig. 7). The U-Pb detrital zircon age patterns are quite similar and
631 typical of Gondwana provenance. Grenville-age zircon of ca. 1.0 Ga can be sourced in
632 the Natal–Namaqua belt of the southern Kalahari. Moreover, Hf isotope composition of
633 the Cryogenian to Ediacaran zircon is compatible with sediment sources in the slightly
634 older (650–570 Ma) Brasiliano–Pan-African orogen and EAAO, as proposed by Rapela
635 et al. (2016). In the Saldania Belt the time of sedimentation is bracketed between 557
636 and 552 Ma in the Malmesbury terrane and between 609 and 532 Ma in the outermost
637 autochthonous Boland Zone (Frimmel et al., 2013). In the first case the lower age
638 corresponds to the older Cape Granite suite plutons that intruded the Malmesbury
639 Group. In NW Argentina deposition of the Puncoviscana Formation can less precisely
640 be bracketed between 570 and ca. 537 Ma (Escayola et al., 2011; Casquet et al., 2012).
641 In consequence both the Puncoviscana and the Malmesbury Group sediments were laid
642 down between 570 Ma (probably after 555 Ma) and ca. 537 Ma. However while in the
643 Saldania Belt sedimentation of the Malmesbury Group preceded the Cape Granite suite,
644 i.e., it was older than 552 Ma, in the Puncoviscana case the youngest sediments were
645 deposited at the same time as I-type arc magmatism in the upper plate (Escayola et al.,
646 2011).

647 Remarkably both sedimentary series lack zircon with Rio de la Plata craton ages
648 between 2.02 and 2.26 Ga (Rapela et al., 2007), implying that the craton was probably
649 not adjacent to the sedimentary basin between 570 and 537 Ma. Since Pampean folding
650 and I-type magmatism in the upper plate were synchronous with right-lateral shearing
651 (Iannizzotto et al., 2013; Van Gosen & Prozzi, 2010), this could mean that the Rio de la
652 Plata craton only reached its present relative position after the main tectonothermal
653 event (530–520 Ma) (Verdecchia et al., 2011). Displacement was focused along the
654 Córdoba Fault, a crust-scale strike-slip and geophysical discontinuity correlated with the
655 Transbrasiliano Lineament (Rapela et al., 2007; Ramé & Miró, 2011) (Figs. 1 & 2) and
656 the displacement juxtaposed the high-grade zone of the Pampean orogen with the Rio de
657 la Plata craton. The latter did not undergo Pampean metamorphism thus implying that

658 the lateral displacement was large and final docking was younger than exhumation of
659 the high-grade domain at ca. 520 Ma.

660

661 **8. Conclusions**

662

663 Combining the evidence given above we hypothesize the following evolution for
664 the Pampean/Saldanian orogeny summarized in Fig. 7:

665

666 a) The Puncoviscana Formation and the Malmesbury group were deposited on a
667 continental margin to the south of the Kalahari craton between 570 and 537 Ma
668 and 570 and 552 Ma respectively. Both were probably separated from the
669 autochthonous Boland terrane through the Piketberg–Wellington Fault (Frimmel
670 et al., 2013). Sediments came from sources in the Brasiliano–Pan-African
671 orogenic belt and the EAAO.

672 b) Magmatism started at ca. 552 Ma with intrusion of the Cape Granite Suite S-
673 type granitoids. A cordilleran I-type magmatic arc formed afterwards, between
674 537 and 528 Ma (most ages are ca. 530Ma), coeval with Puncoviscana
675 sedimentation. Magmatism evolved from S-type to I-type and then back to S-
676 type again over time. The later S-type magmatism (between 530 and 520 Ma) is
677 only recognized in the Sierras Pampeanas and NW Argentina. Fast uplift took
678 place by the end of the I-type magmatism producing dacitic volcanism on top of
679 almost coeval, eroded plutonic rocks of the magmatic arc.

680 c) Subduction was oblique with strain distributed in the upper plate. Right-lateral
681 shear-zones controlled magma emplacement. Folding in the upper plate during
682 the subduction stage produced upright folds. Piñán-Llamas and Simpson (2006)
683 invoke a tectonic model that involves the buttressing of scraped-off
684 Puncoviscana Formation over the subducting slab. This model is compatible
685 with our interpretation of the Puncoviscana Formation as formed in a forearc
686 setting along the eastern margin of the Clymene Ocean.

687 d) Metamorphism during the subduction stage was of high *P/T* type as recognized
688 in the Puncoviscana Formation as it evolved from passive margin sediment into
689 a forearc accretionary prism. Age of this metamorphism remains unknown.

690 e) Continental collision started at ca. 530 Ma resulting in juxtaposition of the
691 Puncoviscana Formation/Malmesbury Group upper plate against the MARA

692 continental block. The latter consisted of a Grenvillian basement with
693 Laurentian affinities and a sedimentary cover of Ediacaran to Early Cambrian
694 age (Murra et al., 2016).

695 f) The intermediate Clymene Ocean was consumed and relics of it were preserved
696 defining a paleo-suture in the Sierras de Córdoba. The age of the oceanic crust
697 was estimated as 647 ± 77 Ma by Escayola et al. (2007), which is compatible
698 with a recent estimate of 620 - 635 Ma for the Early Ediacaran marbles of the
699 sedimentary cover to the MARA block (Murra et al., 2016). The oceanic crust
700 was probably overthrust (obducted) onto the platform of MARA before collision
701 in a manner similar to obduction of the Oman ophiolite (Escayola et al., 2011).

702 g) Collision led to strong deformation and metamorphism between 530 and 520
703 Ma, i.e., younger than the I-type magmatic peak. Sedimentary rocks of the
704 MARA platform and the Puncoviscana Formation, respectively on opposite
705 sides of the suture, were folded and dragged down to as deep as 30 km (8 kbar)
706 at temperatures of up to ca. 800°C. This high-T domain is not found in the
707 Saldania Belt because it was transferred to the Pampean belt in the Sierras
708 Pampeanas. We further infer that this domain underwent uplift and detachment
709 with respect to the low-grade domain by 525–520 Ma, along with strongly
710 peraluminous S-type magmatism. The high-grade domain probably became a
711 mantled gneiss-dome. The origin of heat remains elusive: because igneous rocks
712 of that age are minor we suggest that crustal delamination or crustal foundering
713 played a role.

714 h) Juxtaposition of the Rio de la Plata craton with the Pampean belt across the
715 right-lateral Córdoba Fault took place after the high-grade domain was
716 exhumed, i.e., after 520 Ma. The fault was slightly oblique with respect to axis
717 of the Pampean orogen and probably played a major role in separating the
718 Pampean orogen from the Saldania Belt. The timing of docking probably in the
719 late Early to Late Cambrian remains to be precised.

720

721 **Acknowledgements**

722

723 Financial support for this paper was provided by Argentine public grants CONICET
724 PIP0229, FONCYT PICT 2013-0472 and Spanish grants CGL2009-07984 and

725 GR58/08 UCM-Santander. We acknowledge editorial handling by Dr. Gillian Foulger.
726 The paper has benefited from comments by Dr. Hartwig Frimmel.

727

728

729 **References**

730

731 Aceñolaza, F. & Toselli, A., 1981. Geología del Noroeste Argentino. Publicación de la
732 Facultad de Ciencias e Instituto Miguel Lillo, Universidad Nacional de Tucumán,
733 Tucumán, 212 pp.

734 Aceñolaza, F.G. & Aceñolaza, F., 2007. Insights in the Neoproterozoic–Early
735 Cambrian transition of NW Argentina: facies, environments and fossils in the
736 proto-margin of western Gondwana. Geological Society, London, Special
737 Publications, v. 286, 1-13.

738 Aceñolaza, F.G. & Toselli, A., 2009. The Pampean orogen: Ediacaran–Lower Cambrian
739 evolutionary history of Central and Northwest region of Argentina. *In*: Gaucher, C.,
740 Sial, A.N., Halverson, G.P., Frimmel, H.E. (eds.), Neoproterozoic–Cambrian
741 Tectonics, Global Change and Evolution: A Focus on Southwestern Gondwana.
742 Developments in Precambrian Geology, Elsevier, 16, 239–254.

743 Aceñolaza, F.G. & Toselli, A.J., 1976. Consideraciones estratigráficas y tectónicas sobre
744 el Paleozoico inferior del Noroeste Argentino. Memorias Segundo Congreso
745 Latinoamericano Geología, Caracas, vol. 2, 755–764.

746 Aceñolaza, F.G. & Toselli, A.J., 1973. Consideraciones estratigráficas y tectónicas sobre
747 el Paleozoico Inferior del Noroeste Argentino. In Congreso Latinoamericano de
748 Geología Caracas, vol. 2, 755-783.

749 Adams, C., Miller, H. & Toselli, A.J., & Griffin, W.L., 2008. The Puncoviscana
750 Formation of northwest Argentina: U-Pb geochronology of detrital zircon and Rb-
751 Sr metamorphic ages and their bearing on its stratigraphic age, sediment
752 provenance and tectonic setting. Neues Jahrbuch für Geologie und Paläontologie
753 Abhandlungen, 247, 341-352.

754 Adams, C. J., Miller, H., Aceñolaza, F. G., Toselli, A. J., & Griffin, W. L., 2011. The
755 Pacific Gondwana margin in the late Neoproterozoic–early Paleozoic: detrital
756 zircon U–Pb ages from metasediments in northwest Argentina reveal their
757 maximum age, provenance and tectonic setting. Gondwana Research, 19, 71-83.

758 Anzil, P.A. & Martino, R.D., 2012. Petrografía y geoquímica de las anfibolitas del cerro
759 La Cocha, Sierra Chica, Córdoba. Revista de la Asociación Geológica Argentina,
760 69, 263-274.

761 Aparicio González, P. A., Pimentel, M. M. & Hauser, N., 2011. Datación U-Pb por LA-
762 ICP-MS de diques graníticos del ciclo pampeano, sierra de Mojotoro, Cordillera
763 Oriental. Revista de la Asociación Geológica Argentina, 68, 33-38.

764 Aparicio González, P.A., Pimentel, M.M., Hauser, N. & Moya, M.C., 2014. U-Pb LA-
765 ICP-MS geochronology of detrital zircon grains from low-grade metasedimentary

- 766 rocks (Neoproterozoic – Cambrian) of the Mojotoro Range, northwest Argentina.
767 *Journal of South American Earth Sciences*, 49, 39-59.
- 768 Armstrong, R., De Wit, J., Reid, D., York, D. & Zartman, R. 1998. Cape Town's Table
769 Mountain reveals rapid Pan-African uplift of its basement rocks. *Journal of African*
770 *Earth Sciences*, 27, 10–11.
- 771 Augustsson, C., Willner, A.P., Rüsing, T., Niemeyer, H., Gerdes, A., Adams, C.J. &
772 Miller, H. 2016 The crustal evolution of South America from a zircon Hf-isotope
773 perspective. *Terra Nova*, 28, 128–137.
- 774 Baldo E.G., Rapela, C.W., Pankhurst, R. J., Galindo, C., Casquet, C., Verdecchia, S. O.
775 & Murra, J., 2014, Geocronología de las Sierras de Córdoba: revisión y
776 comentarios. *In: La Geología y Recursos Naturales de la Provincia de Córdoba.*
777 *Relatorio del 19º Congreso Geológico Argentino. Córdoba. Asociación Geológica*
778 *Argentina*, 845 – 870.
- 779 Baldo, E.G., Demange, M. & Martino, R.D. 1996. Evolution of the Sierras de Córdoba,
780 Argentina. *Tectonophysics*, 267, 121-142.
- 781 Bock, B., Bahlburg, H., Wörner, G. & Zimmerman, U. 2000. Tracing crustal evolution
782 in the southern central Andes from Late Precambrian to Permian with geochemical
783 and Nd and Pb isotope data. *The Journal of Geology*, 2000, 108, 515–535.
- 784 Buggisch, W., Kleinschmidt, G., Krumm, F., 2010. Sedimentology, geochemistry and
785 tectonic setting of the Neoproterozoic Malmesbury Group (Tygerberg Terrane) and
786 its relation to neighboring terranes, Saldania Fold Belt, South Africa. *Neues*
787 *Jahrbuch für Geologie und Paläontologie*, 257, 85-114.
- 788 Casquet, C., Pankhurst, R.J., Galindo, C., Rapela, C., Fanning, M., Baldo, E., Dahlquist,
789 J., González Casado, J. & Colombo, F., 2012. A History of proterozoic terranes in
790 southern south America: From Rodinia to Gondwana. *Geosciences Frontiers*, 3,
791 137-145.
- 792 Chemale, F., Scheepers, R., Gresse, P. G., & Van Schmus, W. R. 2011. Geochronology
793 and sources of late Neoproterozoic to Cambrian granites of the Saldania Belt.
794 *International Journal of Earth Sciences*, 100, 431-444.
- 795 Cordani, U. G., D'Agrella-Filho, M.S., Brito-Neves, B.B. & Trindade, R.I.F., 2003.
796 Tearing up Rodinia: the Neoproterozoic palaeogeography of South American
797 cratonic fragments *Terra Nova*, 15, 350–359.
- 798 Curtis, M.L., 2001 Tectonic history of the Ellsworth Mountains, West Antarctica:
799 reconciling a Gondwana enigma. *Geological Society of America Bulletin*, 113, 939-
800 958.
- 801 Da Silva, L.C., Gresse, P.G., Scheepers, R., McNaughton, N.J., Hartmann, L.A. &
802 Fletcher, I., 2000. U-Pb SHRIMP and Sm-Nd age constraints on the timing and
803 sources of the Pan-African Cape Granite Suite, South Africa. *Journal of African*
804 *Earth Sciences*, 30, 795-815.
- 805 Dahlquist, J. A., Verdecchia, S. O., Baldo, E. G., Basei, M. A., Alasino, P. H., Urán, G.
806 A., Rapela, C.W., Campos Neto, M.C. & Zandomeni, P. S., 2016. Early Cambrian
807 U-Pb zircon age and Hf-isotope data from the Guasayán pluton, Sierras Pampeanas,

- 808 Argentina: implications for the northwestern boundary of the Pampean arc. *Andean*
809 *Geology*, 43, 137-150.
- 810 Dalziel, I.W.D., 1997. Overview. Neoproterozoic–Paleozoic geography and tectonics:
811 review, hypothesis, environmental speculation. *Geological Society of America*.
812 *Bulletin* 109, 16–42.
- 813 Do Campo, M. & Guevara, S. R., 2005. Provenance analysis and tectonic setting of late
814 Neoproterozoic metasedimentary successions in NW Argentina. *Journal of South*
815 *American Earth Sciences*, 19, 143-153.
- 816 Do Campo, M. & Nieto, F., 2003. Transmission electron microscopy study of very low-
817 grade metamorphic evolution in Neoproterozoic pelites of the Puncoviscana
818 formation (Cordillera Oriental, NW Argentina). *Clay Minerals*, 38, 459-481.
- 819 Do Campo, M., Collo, G. & Nieto, F., 2013. Geothermobarometry of very low-grade
820 metamorphic pelites of the Vendian–Early Cambrian Puncoviscana Formation (NW
821 Argentina). *European Journal of Mineralogy*, 25, 429-451.
- 822 Drobe, M., López de Luchi, M. G., Steenken, A., Frei, R., Naumann, R., Siegesmund, S.
823 & Wemmer, K., 2009. Provenance of the late Proterozoic to early Cambrian
824 metaclastic sediments of the Sierra de San Luis (Eastern Sierras Pampeanas) and
825 cordillera Oriental, Argentina. *Journal of South American Earth Sciences*, 28, 239-
826 262.
- 827 Escayola M.P., Pimentel, M.M. & Armstrong, R., 2007. Neoproterozoic back arc basin:
828 sensitive high-resolution ion microprobe U–Pb and Sm–Nd isotopic evidence from
829 eastern Pampean ranges, Argentina. *Geology*, 35: 495–498.
- 830 Escayola, M.P., van Staal, C.R. & Davis, W.J., 2011. The age and tectonic setting of the
831 Puncoviscana Formation in northwestern Argentina: an accretionary complex related
832 to Early Cambrian closure of the Puncoviscana Ocean and accretion of the
833 Arequipa-Antofalla block. *Journal of South American Earth Sciences* 32: 438-459.
- 834 Farina, F., Stevens, G., Gerdes, A. & Frei, D., 2014. Small-scale Hf isotopic variability
835 in the Peninsula pluton (South Africa): the processes that control inheritance of
836 source $^{176}\text{Hf}/^{177}\text{Hf}$ diversity in S-type granites. *Contributions to Mineralogy and*
837 *Petrology*, 168:1065. doi 10.1007/s00410-014-1065-8
- 838 Favetto, A., Pomposiello, C., López de Luqui, M.G. & Booker, J., 2008. 2D
839 Magnetotelluric interpretation of the crust electrical resistivity across the Pampean
840 terrane–Río de la Plata suture, in central Argentina. *Tectonophysics* 2008, 459 (1-4)
841 54-65.
- 842 Frimmel, H.E., Basei, M.A.S., Correa, V.X. & Mbangula, N., 2013. A new
843 lithostratigraphic subdivision and geodynamic model for the Pan-African western
844 Saldania Belt, South Africa *Precambrian Research*, 231, 218-235.
- 845 Gorayeb, P.S.S., Chaves, C.L., Veloso Moura, C.A. & da Silva Lobo, L.R., 2013.
846 Neoproterozoic granites of the Lajeado intrusive suite, north-center Brazil: A late
847 Ediacaran remelting of a Paleoproterozoic crust. *Journal of South American Earth*
848 *Sciences*, 45, 278-292.

- 849 Gordillo, C.E. & Lencinas, A. N., 1979. Sierras Pampeanas de Córdoba y San Luis.
850 *Segundo Simposio de Geología Regional Argentina*, Academia Nacional de
851 Ciencias, Córdoba, 2, 577-650.
- 852 Gromet, L. P., Otamendi, J. E., Miró, R. C., Demichelis, A. H., Schwartz, J. J. &
853 Tibaldi, A. M., 2005. The Pampean orogeny: ridge subduction or continental
854 collision. *Gondwana 12 Symposium*, Mendoza, Argentina, Abs. 185.
- 855 Guerreschi, A. B. & Martino, R. D., 2014. Las migmatitas de Sierras de Córdoba. *In: La*
856 *Geología y Recursos Naturales de la Provincia de Córdoba. Relatorio del 19°*
857 *Congreso Geológico Argentino*, Córdoba. Asociación Geológica Argentina, 67-94.
- 858 Hauser, N., Matteini, M., Omarini, R.H. & Pimentel, M.M., 2011; Combined U–Pb and
859 Lu–Hf isotope data on turbidites of the Paleozoic basement of NW Argentina and
860 petrology of associated igneous rocks: Implications for the tectonic evolution of
861 western Gondwana between 560 and 460Ma. *Gondwana Research*, 19, 100-127.
- 862 Hervé, F., Calderón, M., Fanning, C.M., Kraus, S. & Pankhurst, R.J., 2010. SHRIMP
863 chronology of the Magallanes basin basement, Tierra del Fuego: Cambrian
864 plutonism and Permian high-grade metamorphism. *Andean Geology*, 37, 253-275.
- 865 Hongn, F. D., Tubía, J. M., Aranguren, A., Vegas, N., Mon, R. & Dunning, G. R., 2010.
866 Magmatism coeval with lower Paleozoic shelf basins in NW-Argentina (Tastil
867 batholith): constraints on current stratigraphic and tectonic interpretations. *Journal*
868 *of South American Earth Sciences*, 29, 289-305.
- 869 Iannizzotto, N.F., Rapela, C.W., Baldo, E.G., Galindo, C. & Fanning, C.M., 2013. The
870 Sierra Norte–Ambargasta Batholith: Cambrian magmatism formed in a
871 transpressional belt along the western edge of the Río de la Plata cratón? *Journal of*
872 *South American Earth Sciences*, 42, 127-142.
- 873 Jacobs, J. & Thomas, R.J., 2004. Himalayan-type indenter-escape tectonics model for
874 the southern part of the late Neoproterozoic–early Paleozoic East African–
875 Antarctic orogen. *Geology*, 32, 721-724.
- 876 Jezek, P., 1990. Análisis sedimentológico de la Formación Puncoviscana entre Tucumán
877 y Salta. *El Ciclo Pampeano en el Noroeste Argentino. Serie Correlación Geológica*
878 *(INSUGEO-CONICET-UNT)*, 4, 9-36.
- 879 Kraemer, P.E., Escayola, M.P. & Martino, R.D., 1995. Hipótesis sobre la evolución
880 tectónica neoproterozoica de las Sierras Pampeanas de Córdoba (30° 40' – 32° 40')
881 Argentina. *Revista de la Sociedad Geológica Argentina*, 50, 47-59.
- 882 Kristoffersen, M., Andersen, T. & Elburg, M.A., 2016. Detrital zircon in a
883 supercontinental setting: locally derived and far-transported components in the
884 Ordovician Natal Group, South Africa. *Journal of the Geological Society, London.*
885 173, 203-215.
- 886 Leal, P.R., Hartmann, L.A., Jos, S., Miró, R.C. & Ramos, V.A., 2003. Volcanismo
887 postorogénico en el extremo norte de las Sierras Pampeanas Orientales: Nuevos
888 datos geocronológicos y sus implicancias tectónicas. *Revista de la Asociación*
889 *Geológica Argentina*, 58, 593-607.
- 890 Lucassen, F., Becchio, R., Wilke, H. G., Franz, G., Thirlwall, M. F., Viramonte, J. &
891 Wemmer, K., 2000. Proterozoic–Paleozoic development of the basement of the

- 892 Central Andes (18–26 S)—a mobile belt of the South American craton. *Journal of*
893 *South American Earth Sciences*, 13, 697-715.
- 894 Lyons, P., Skirrow, R. G. & Stuart-Smith, P. G., 1997. Geology and Metallogeny of the
895 Sierras Septentrionales de Córdoba. 1; 250.000 map sheet, Province of Córdoba.
896 Geoscientific mapping of the Sierras Pampeanas Argentine-Australia Cooperative
897 Project. *Servicio Geológico Minero Argentino. Anales*, 27, 1-131.
- 898 Martino, R., Kraemer, P., Escayola, M., Giambastiani, M. & Arnosio, M., 1995.
899 Transecta de las sierras Pampeanas de Córdoba a los 32° LS. *Revista de la*
900 *Asociación Geológica Argentina*, 50, 60-77.
- 901 Martino, R., Pinceyra, R., Guerreschi, A. & Sfragulla, J., 1999. La faja de deformación
902 Sauce Punco, Sierra Norte, Córdoba, Argentina. *Revista de la Asociación Geológica*
903 *Argentina* 53, 436–440.
- 904 Martino, R., Simpson, C. & Law, R., 1994. Ductile thrusting in Pampean Ranges: Its
905 relationships with the Oclayic deformation and tectonic significance. *International*
906 *Geological Correlation Programme, Project 376. Laurentian-Gondwanan*
907 *Connections before Pangea. Nova Scotia, Canadá.*
- 908 Martino, R.D., Guerreschi, A.B. & Anzil, P.A., 2010. Metamorphic and tectonic
909 evolution at 31°36'S across a deep crustal zone from the Sierra Chica of Córdoba,
910 Sierras Pampeanas, Argentina, *Journal of South American Earth Sciences*, 30, 12-
911 28.
- 912 Martino, R.D., Guerreschi, A.B. & Sfragulla, J.A., 2003. Petrography, structure and
913 tectonic significance of 'Los Túneles' Shear Zone, Sierras de Pocho y Guasapampa,
914 Córdoba, Argentina. *Revista de la Asociación Geologica Argentina*, 58, 233-247.
- 915 Martino, R., 2003. Las fajas de deformación dúctil de las Sierras Pampeanas de
916 Córdoba: Una reseña general *Revista de la Asociación Geológica Argentina*, 58,
917 549–571.
- 918 Murra, J. A., Casquet, C., Locati, F., Galindo, C., Baldo, E.G., Pankhurst, R.J. & Rapela,
919 C.W., 2016. Isotope (Sr, C) and U–Pb SHRIMP zircon geochronology of marble-
920 bearing sedimentary series in the Eastern Sierras Pampeanas, Argentina.
921 Constraining the SW Gondwana margin in Ediacaran to early Cambrian times.
922 *Precambrian Research*, 281, 602-617.
- 923 Naidoo, T., Zimmermann, U. & Chemale, F., 2013. The evolution of Gondwana: U–Pb,
924 Sm–Nd, Pb–Pb and geochemical data from Neoproterozoic to Early Palaeozoic
925 successions of the Kango Inlier (Saldania Belt, South Africa). *Sedimentary*
926 *Geology*, 294, 164-178.
- 927 Omarini, R., Sureda, R., Götze, H., Seilacher, A. & Plüger, F., 1999. The Puncoviscana
928 folded belt: A testimony of late Proterozoic Rodinia fragmentation and the
929 collisional pre-Gondwanic episodes. *Geologische Rundschau*, 88, 76–97.
- 930 Otamendi, J. E., Tibaldi, A. M., Vujovich, G. I. & Viñao, G. A., 2008. Metamorphic
931 evolution of migmatites from the deep Famatinian arc crust exposed in Sierras Valle
932 Fértil–La Huerta, San Juan, Argentina. *Journal of South American Earth Sciences*,
933 25, 313-335.

- 934 Otamendi, J.E., Patiño Douce, A.E. & Demichelis, A.H., 1999. Amphibolite to granulite
935 transition in aluminous greywackes from the sierra de Comechingones, Córdoba,
936 Argentina. *Journal of Metamorphic Geology*, 17, 415-434.
- 937 Otamendi, J.E., Tibaldi, A.M., Demichelis, A. H. & Rabbia, O.M., 2005. Metamorphic
938 evolution of the Río Santa Rosa Granulites, northern Sierra de Comechingones,
939 Argentina. *Journal of South American Earth Sciences*, 18, 163-181.
- 940 Pankhurst, R.J., Rapela, C.W., López de Luchi, M.G., Rapalini, A.E., Fanning, C.M. &
941 Galindo, C., 2014. The Gondwana connections of Patagonia. *Journal of the
942 Geological Society, London*, 171, 313–328.
- 943 Peri, V.G., Pomposiello, M.C., Favetto, A., Barcelona, H. & Rossello, E.A., 2013.
944 Magnetotelluric evidence of the tectonic boundary between the Río de La Plata
945 Craton and the Pampean terrane (Chaco-Pampean Plain, Argentina): The extension
946 of the Transbrasiliano Lineament. *Tectonophysics*, 608, 685–699.
- 947 Piñán-Llamas, A. & Escamilla-Casas, J.C., 2013. Provenance and tectonic setting of
948 Neoproterozoic to Early Cambrian metasedimentary rocks from the Cordillera
949 Oriental and Eastern Sierras Pampeanas, NW Argentina. *Boletín de la Sociedad
950 Geológica Mexicana*, 65, 373-395.
- 951 Piñán-Llamas, A. & Simpson, C., 2006. Deformation of Gondwana margin turbidites
952 during the Pampean orogeny, north-central Argentina. *Geological Society of
953 America Bulletin*, 118, 1270-1279.
- 954 Proenza, J.A., Zaccarini, F., Escayola, M., Cábana, C., Schalamuk, A. & Garuti, G.,
955 2008. Composition and textures of chromite and platinum-group minerals in
956 chromitites of the western ophiolitic belt from Pampean Ranges of Córdoba,
957 Argentina. *Ore Geology Reviews*, 33, 32-48.
- 958 Ramacciotti, C.D., Baldo, E.G. & Casquet, C., 2015. U–Pb SHRIMP detrital zircon ages
959 from the Neoproterozoic Difunta Correa Metasedimentary Sequence (Western
960 Sierras Pampeanas, Argentina): Provenance and paleogeographic implications.
961 *Precambrian Research*, 270, 39-49.
- 962 Ramé, G.A. & Miró, R.C., 2011. Modelo geofísico de contacto entre el Orógeno
963 Pampeano y el Cratón del Río de La Plata en las provincias de Córdoba y Santiago
964 del Estero. *Serie de Correlación Geológica (INSUGEO-CONICET-UNT)*, 27,
965 111-123.
- 966 Ramos, V.A., 1988. Tectonics of the Late-Proterozoic–Early Paleozoic: a collisional
967 history of southern South America. *Episodes*, 11, 168–174.
- 968 Ramos, V.A., Escayola, M., Mutti, D.I. & Vujovich, G.I., 2000. Proterozoic–early
969 Paleozoic ophiolites of the Andean basement of southern South America.
970 *Geological Society of America Special Paper*, 349, 331–349.
- 971 Ramos, V.A., Escayola, M., Leal, P., Pimentel, M.M., Santos, J.O., 2015. The late stages
972 of the Pampean Orogeny, Cordoba (Argentina): Evidence of postcollisional Early
973 Cambrian slab break-off magmatism. *Journal of South American Earth Sciences*,
974 64, 351-364.
- 975 Ramos, V.A., Vujovich, G., Martino, R. & Otamendi, J., 2010. Pampia: a large cratonic
976 block missing in the Rodinia supercontinent. *Journal of Geodynamics* 50, 243–255.

- 977 Rapela C.W., Baldo E.G, Pankhurst R.J. & Saavedra J., 2002. Cordieritite and
978 Leucogranite Formation during Emplacement of Highly Peraluminous Magma: the
979 El Pilón Granite Complex (Sierras Pampeanas, Argentina). *Journal of Petrology* 43,
980 1003–1028.
- 981 Rapela C.W., Pankhurst R.J., Casquet C., Baldo E., Saavedra J., Galindo C. & Fanning
982 C.M., 1998. The Pampean Orogeny of the south proto-Andes: evidence for
983 Cambrian continental collision in the Sierras de Cordoba. *In*: R.J. Pankhurst R.J. &
984 C.W. Rapela (Eds.). *The proto-Andean Margin of Gondwana*. Special Publication
985 Geological Society, London, 142, 181–217.
- 986 Rapela, C.W., Fanning, C.M., Casquet, C., Pankhurst, R.J., Spalletti, L., Poiré, D.,
987 Baldo, E.G., 2011. The Rio de la Plata craton and the adjoining Pan-
988 African/Brasiliano terranes: Their origins and incorporation into south west
989 Gondwana. *Gondwana Research*, 20, 673–690. doi:10.1016/j.gr.2011.05.001.
- 990 Rapela, C.W., Pankhurst, R.J., Casquet, C., Fanning, C.M., Baldo, E.G., González-
991 Casado, J.M., Galindo, C. & Dahlquist, J., 2007. The Río de la Plata craton and the
992 assembly of SW Gondwana. *Earth Science Review*, 83, 49-82.
- 993 Rapela, C.W., Pankhurst, R.J., Fanning, C.M. & Grecco, L.E., 2003. Basement
994 evolution of the Sierra de la Ventana Fold Belt: new evidence for Cambrian
995 continental rifting along the southern margin of Gondwana. *Journal of the*
996 *Geological Society*, London 160, 613–628.
- 997 Rapela, C.W., Verdecchia, S.O., Casquet, C., Pankhurst, R.J., Baldo, E.G., Galindo, C.,
998 Murra, J.A., Dahlquist, J.A. & Fanning, C.M., 2016. Identifying Laurentian and
999 SW Gondwana sources in the Neoproterozoic to Early Paleozoic metasedimentary
1000 rocks of the Sierras Pampeanas: Paleogeographic and tectonic implications.
1001 *Gondwana research*, 32, 193-212.
- 1002 Rowe, C.D., Backeberg, N.R., Van Rensburg, T., Maclennan, S.A., Faber, C., Curtis,
1003 C., Viglietti, P.A., 2010. Structural geology of Robben Island: implications for the
1004 tectonic environment of Saldanian deformation. *South African Journal of Geology*,
1005 2010, 113, 57-72. doi:10.2113/Gssajg.113.1-57.
- 1006 Rozendaal, A., Gresse, P.G, Scheepers, R. & Le Roux, J.P., 1999 Neoproterozoic to
1007 Early Cambrian Crustal Evolution of the Pan-African Saldania Belt, South Africa.
1008 *Precambrian Research*, 97, 303-323.
- 1009 Scheepers R. & Armstrong, R., 2002. New U-Pb SHRIMP zircon ages of the Cape
1010 Granite Suite: implications for the magmatic evolution of the Saldania Belt. *South*
1011 *African Journal of Geology*, 105, 241-256.
- 1012 Scheepers, R. & Poujol, M., 2002. U-Pb zircon age of Cape Granite Suite ignimbrites:
1013 characteristics of the last phases of the Saldanian magmatism. *South African*
1014 *Journal of Geology*, 105, 163-178.
- 1015 Scheepers, R., 1995. Geology, Geochemistry and petrogenesis of late Precambrian S, I
1016 and A-type granitoids in the Saldania Mobile Belt, Southwestern Cape Province.
1017 *Journal of African Earth Science*, 21, 35-58.
- 1018 Schobbenhaus Filho, C., 1975. Folha Goiás. SD. 22. Carta Geológica do Brasil ao
1019 Milionésimo, Folha Goiás (SD22). DNPM, Brasília.

- 1020 Schwartz, J.J. & Gromet, L.P., 2004. Provenance of Late Proterozoic-early Cambrian
1021 basin, Sierras de Córdoba, Argentina. *Precambrian Research*, 129, 1–21.
- 1022 Schwartz, J.J., Gromet, L.P. & Miró, R., 2008. Timing and Duration of the Calc-
1023 Alkaline Arc of the Pampean Orogeny: Implications for the Late Neoproterozoic to
1024 Cambrian Evolution of Western Gondwana. *Journal of Geology*, 116:39–61.
- 1025 Siegesmund, S., Steenken, A., Martino, R., Wemmer, K., López de Luchi, M.G., Frei,
1026 R., Presnyakow, S. & Guerschi, A., 2010. Time constraints on the tectonic
1027 Evolution of the Eastern Sierras Pampeanas (Central Argentina). *International*
1028 *Journal Earth Sciences* 99: 1199-1226.
- 1029 Söllner, F., Leal, P.R., Miller, H. & Brodtkorb, M.K., 2000. Edades U/Pb en circones de
1030 la riodacita de la Sierra de Ambargasta, provincia de Córdoba. *In: I. Schalamuk,*
1031 *M.K. Brodtkorb & R. Etcheverry, R. (Eds.), Mineralogía y Metalogenia 2000,*
1032 *INREMI, La Plata, Publicación, 6, 465- 469.*
- 1033 Spagnuolo, C. M., Rapalini, A. E. & Astini, R. A., 2012. Assembly of Pampia to the SW
1034 Gondwana margin: A case of strike-slip docking? *Gondwana Research*, 21, 406-
1035 421.
- 1036 Steenken A., Wemmer, K., Martino, R.D., López de Luchi, M.G., Guereschi, A. &
1037 Siegesmund, S., 2010. Post-Pampean cooling and the exhumation of the Sierras
1038 Pampeanas in the West of Córdoba. (Central Argentina). *Neues Jahrbuch für*
1039 *Geologie und Paläontologie*, 256, 235-255.
- 1040 Steenken, A., Siegesmund, S., López de Luqui, M.G., Frei, R. & Wemmer, K., 2006.
1041 Neoproterozoic to Early Palaeozoic events in the Sierra de San Luis: implications
1042 for the Famatinian geodynamics in the Eastern Sierras Pampeanas (Argentina).
1043 *Journal of the Geological Society, London*, 163, 965-982.
- 1044 Stuart-Smith, P. G., Miró, R., Sims, J. P., Pieters, P. E., Lyons, P., Camacho, A. & Black,
1045 L. P., 1999. Uranium-lead dating of felsic magmatic cycles in the southern Sierras
1046 Pampeanas, Argentina: implications for the tectonic development of the proto-
1047 Andean Gondwana margin. *Special Papers. Geological Society of America*, 87-114.
- 1048 Thomas, R.J., Jacobs, J., Horstwood, M.S., Ueda, K., Bingen, B. & Matola, R., 2010.
1049 The Mecubúri and Alto Benfica Groups, NE Mozambique: aids to unravelling *ca.* 1
1050 and 0.5 Ga events in the East African orogen. *Precambrian Research*, 178, 72–90.
- 1051 Tibaldi, A. M., Otamendi J.E., Gromet, L.P. & Demichelis, A. H., 2008. Suya Taco and
1052 Sol de Mayo mafic complexes from eastern Sierras Pampeanas, Argentina:
1053 Evidence for the emplacement of primitive OIB-like magmas into deep crustal
1054 levels at a late stage of the Pampean orogeny. *Journal of South American Earth*
1055 *Sciences* 26, 172-187.
- 1056 Trindade, R.I.F., D'Agrella-Filho, M.S., Epof, I. & Brito Neves, B.B., 2006.
1057 Paleomagnetism of Early Cambrian Itabaiana mafic dikes (NE Brazil) and the final
1058 assembly of Gondwana. *Earth Planet Science Letters*, 244, 361–377.
- 1059 Verdecchia S.O., Reche J., Baldo E.G., Segovia-Díaz E. & Martínez F.J., 2012.
1060 Staurolite porphyroblast controls on local bulk compositional and microstructural
1061 changes during decompression of a St-Bt-Grt-Crd-And schist (Ancasti
1062 metamorphic complex, Sierras Pampeanas, W Argentina). *Journal of Metamorphic*
1063 *Geology*, 31, 131-146.

- 1064 Verdecchia, S.O., Casquet, C., Baldo, E.G., Pankhurst, R.J., Rapela, C.W., Fanning,
 1065 C.M. & Galindo, C., 2011. Mid- to Late Cambrian docking of the Rio de la Plata
 1066 craton to southwestern Gondwana: age constraints from U–Pb SHRIMP detrital
 1067 zircon ages from Sierras de Ambato and Velasco (Sierras Pampeanas, Argentina).
 1068 *Journal of the Geological Society, London*, 168, 1061–1071.
- 1069 Villaros, A., Buick, I. S. & Stevens, G., 2012. Isotopic variations in S-type granites: an
 1070 inheritance from a heterogeneous source? *Contributions to Mineralogy and*
 1071 *Petrology*, 163, 243–257.
- 1072 von Gosen, W. & Prozzi, C., 2010. Pampean deformation in the Sierra Norte de
 1073 Córdoba, Argentina: implications for the collisional history at the western pre-
 1074 Andean Gondwana margin. *Tectonics*, 29, 1–33.
- 1075 von Gosen, W., McClelland, W.C., Loske, W., Martínez, J.C. & Prozzi, C., 2014.
 1076 Geochronology of igneous rocks in the Sierra Norte de Córdoba (Argentina):
 1077 implications for the Pampean evolution at the western Gondwana margin.
 1078 *Lithosphere*, 6, 277–300.
- 1079 Warr, L.N. & Ferreiro Mählmann, R., 2015. Recommendations for Kübler Index
 1080 standardization. *Clay Minerals*. 50, 283–286.
- 1081 Whitmeyer, J.S. & Simpson, C., 2003. High strain-rate deformation fabrics characterize
 1082 a kilometers thick Paleozoic fault zone in the Eastern Sierras Pampeanas, Central
 1083 Argentina. *Journal of Structural Geology*, 25, 904–922.
- 1084 Willner, A.P., Toselli, A.J., Basán, C. & Vides de Bazán, M.E., 1983. Rocas
 1085 metamórficas. In Aceñolaza, F.G., Miller, H. & Toselli, A (Eds.), *La geología de la*
 1086 *Sierra de Ancasti*. Munstersche Forschungen zur Geologie und Paleontologie,
 1087 *Munster*, 59, 31–78.
- 1088 Yin, A., 2004. Gneiss domes and gneiss dome systems, in Whitney, D.L., Teyssier, C.,
 1089 and Siddoway, C.S., eds., *Gneiss domes in orogeny: Boulder, Colorado*, Geological
 1090 *Society of America Special Paper*, 380, 1–14.
- 1091 Zimmermann, U., 2005. Provenance studies of very low- to low-grade metasedimentary
 1092 rocks of the Puncoviscana complex, northwest Argentina. In: Vaughan, A.P.M.,
 1093 Leat, P.T. & Pankhurst, R.J. (eds) *Terrane Processes at the Margins of Gondwana*,
 1094 *Geological Society, London, Special Publication*, 246, 381–416.

1095
 1096

1097 **Figure Captions**

1098

1099 Fig. 1. Schematic geological map of South America showing Paleoproterozoic to
 1100 Archean cratons, Mesoproterozoic mobile belts, and the Neoproterozoic-to-early
 1101 Cambrian orogens.

1102

1103 Fig. 2. Schematic geological map of the Sierras Pampeanas showing the Pampean belt
 1104 (ca. 545–520 Ma) and the Ordovician accretionary-type Famatinian belt (490–440Ma).
 1105 The inferred Pampean suture is indicated. Ruled decoration shows Pampean orogen
 1106 reworked by the Famatinian orogeny. NWA is North Western Argentina. CP: Carapé
 1107 Fault (Martino, 2003).

1108

1109 Fig. 3. Schematic cross-section of the Pampean orogen sandwiched between the
1110 Paleoproterozoic Rio de la Plata craton (RPC) and the Ordovician Famatinian orogen.
1111

1112 Fig. 4. Probability plot with histograms and TW plots of samples from the Puncoviscana
1113 Formation-equivalent Pocho Phyllites (TLT-2069) and the Malmesbury Group (HFS08-
1114 06; Frimmel et al., 2013) from the Saldanian orogen in South Africa.
1115

1116 Fig. 5. Plot of P-T conditions of Pampean metamorphism recovered from conventional
1117 thermobarometry by different authors (see footnote for references). M2 and M3 events
1118 in migmatites, gneisses and granulites from (a) Do Campo et al. (2013), (b, c) Rapela et
1119 al. (1998), (d, e) Rapela et al.(2002), (f, g, h) Otamendi et al.(1999), (i) Otamendi et al.
1120 (2005), (j) (Martino et al. (2010). M2 conditions are shown as white boxes and circles
1121 and black line, whereas grey boxes and black circles represent M₃ conditions. The
1122 broken lines join thermobarometric calculations made on the same metamorphic rocks.
1123 Where uncertainties are available they are indicated. The thick dashed curves embrace
1124 the probable clockwise metamorphic P-T path for both the low-grade high-P domain
1125 and the high-grade domain.
1126

1127 Fig. 6. Plot of ϵ_{Hf} values vs. age of detrital zircon between 570 and 700 Ma from the
1128 Puncoviscana Formation of NW Argentina (Hauser et al., 2011; Augustsson et al.,
1129 2016), sample TLT-2069 from this work (Table 2), the Saldanian belt (Frimmel et al.,
1130 2013) and the Mecuburí Group of the East Africa-Antarctica Orogen (Thomas et al.,
1131 2010).
1132

1133 Fig. 7. Paleogeographic and dynamic model for the origin and evolution of the
1134 Pampean–Saldanian orogeny. Modified after Rapela et al. (2007). The orogeny resulted
1135 from oblique subduction of the Clymene Ocean beneath a continental margin with right-
1136 laterally displacement relative to the Kalahari and Rio de la Plata cratons. A) The
1137 margin was fed with turbidite sediments (Puncoviscana Formation and Malmesbury
1138 Group) derived from the erosion of the Neoproterozoic large East African-Antarctica
1139 Orogen in the east and the Brasiliano–Pan-African orogens in the west. Displacement
1140 was focused along an earlier continent-scale fault (probably a transform fault). B) The
1141 margin became active and magmatic arcs developed (S-type and I-type) between 552
1142 and 530 Ma. Sedimentation of the Puncoviscana Formation continued in the forearc as
1143 an accretionary prism. C) Closure of the Clymene Ocean at ca. 530 Ma brought arc
1144 magmatism to an end and resulted in continental collision between MARA (that had
1145 formerly rifted away from Laurentia) and the active margin between ca. 530 and 520
1146 Ma. High P/T metamorphism is recorded from the upper plate while intermediate to low
1147 P/T metamorphism took place in the lower plate. An obducted ophiolite in the Sierras
1148 Pampeanas is evidence for the continental suture. Collision took place along with
1149 continuous right-lateral displacement of the closed margin. The resulting transpressional
1150 orogen was westward vergent (westward and upright folds in the Pampean belt; upright
1151 to weakly westward folds in the Saldanian belt). D) The Pampean orogen records uplift
1152 between 525 and 520 Ma. Renewed right-lateral movement along the Córdoba Fault
1153 eventually juxtaposed the Rio de la Plata craton against the internal part of the Pampean
1154 orogen. This fault strikes at a low angle relative to the orogenic grain, suggesting that it
1155 played a major role in the detachment of the Pampean belt from the Saldanian belt.
1156

Grain. spot	U (ppm)	Th (ppm)	Th/U	²⁰⁴ Pb/ ²⁰⁶ Pb	f ₂₀₆ %	Total ratios				Radiogenic Ratios					Ages (in Ma)				% Disc			
						²³⁸ U/ ²⁰⁶ Pb	²⁰⁶ Pb/ ±	²⁰⁷ Pb/ ±	²⁰⁶ Pb/ ±	²⁰⁶ Pb/ ²³⁸ U	²⁰⁷ Pb/ ±	²⁰⁷ Pb/ ²³⁵ U	²⁰⁷ Pb/ ²⁰⁶ Pb	²⁰⁶ Pb/ ²³⁸ U	²⁰⁷ Pb/ ²³⁵ U	²⁰⁷ Pb/ ²⁰⁶ Pb	±	±		±	±	
1.1	217	107	0.49	#####	0.19	9.867	0.147	0.0620	0.0007	0.1012	0.0015					621	9					
2.1	436	95	0.22	#####	0.14	10.074	0.132	0.0616	0.0005	0.0991	0.0013					609	8					
3.1	215	115	0.54	#####	0.21	9.021	0.154	0.0639	0.0009	0.1106	0.0019					676	11					
3.2	272	186	0.68	-	0.07	10.065	0.133	0.0610	0.0010	0.0993	0.0013					610	8					
4.1	533	48	0.09	#####	0.00	5.950	0.074	0.0747	0.0005	0.1681	0.0021	1.730	0.026	0.0747	#####	1001	12	1020	10	1059	14	5
5.1	389	109	0.28	#####	0.18	5.770	0.081	0.0755	0.0010	0.1730	0.0024	1.766	0.041	0.0740	#####	1029	13	1033	15	1042	35	1
6.1	406	203	0.50	#####	0.33	5.721	0.070	0.0748	0.0006	0.1742	0.0021	1.730	0.031	0.0720	#####	1035	12	1020	12	987	24	-5
7.1	267	9	0.03	#####	0.07	9.211	0.142	0.0627	0.0010	0.1085	0.0017					664	10					
8.1	304	<1	<0.01	#####	0.09	10.473	0.142	0.0604	0.0014	0.0954	0.0013					587	8					
9.1	92	77	0.84	-	<0.01	2.186	0.038	0.1646	0.0013	0.4576	0.0080	10.393	0.209	0.1647	#####	2429	36	2470	19	2505	13	3
10.1	67	36	0.53	#####	0.42	10.933	0.333	0.0631	0.0019	0.0911	0.0028					562	16					
11.1	304	100	0.33	-	0.01	9.891	0.153	0.0608	0.0009	0.1011	0.0016					621	9					
12.1	485	57	0.12	#####	0.19	6.636	0.085	0.0703	0.0007	0.1504	0.0019	1.425	0.026	0.0687	#####	903	11	899	11	890	23	-1
13.1	501	108	0.22	#####	0.18	5.977	0.072	0.0743	0.0006	0.1670	0.0020	1.676	0.027	0.0728	#####	996	11	1000	10	1008	19	1
14.1	653	87	0.13	#####	0.07	6.289	0.073	0.0765	0.0005	0.1589	0.0018	1.662	0.024	0.0759	#####	951	10	994	9	1092	14	13
15.1	137	39	0.28	-	<0.01	5.547	0.091	0.0744	0.0010	0.1804	0.0030	1.861	0.042	0.0748	#####	1069	16	1067	15	1064	28	0
16.1	516	253	0.49	#####	0.03	9.723	0.120	0.0613	0.0005	0.1028	0.0013					631	7					
17.1	230	59	0.26	#####	0.10	6.237	0.097	0.0761	0.0010	0.1602	0.0025	1.661	0.038	0.0752	#####	958	14	994	15	1074	30	11
18.1	939	460	0.49	#####	0.32	9.166	0.319	0.0770	0.0005	0.1088	0.0038					666	22					
19.1	537	198	0.37	#####	3.11	17.094	0.800	0.0791	0.0015	0.0567	0.0027					355	16					
20.1	290	89	0.31	#####	0.03	3.165	0.055	0.1153	0.0011	0.3159	0.0055	5.010	0.105	0.1150	#####	1770	27	1821	18	1880	17	6
21.1	488	36	0.07	#####	0.04	5.520	0.072	0.0742	0.0007	0.1811	0.0024	1.845	0.031	0.0739	#####	1073	13	1062	11	1039	18	-3
21.2	275	49	0.18	#####	0.14	5.498	0.070	0.0741	0.0010	0.1816	0.0023	1.826	0.038	0.0729	#####	1076	13	1055	14	1011	31	-6
22.1	562	8	0.01	#####	0.05	7.293	0.095	0.0655	0.0005	0.1371	0.0018	1.230	0.019	0.0651	#####	828	10	814	9	777	15	-7
23.1	153	88	0.58	-	<0.01	5.458	0.085	0.0752	0.0007	0.1835	0.0029	1.929	0.045	0.0763	#####	1086	16	1091	16	1102	31	1
24.1	370	50	0.13	#####	0.00	10.040	0.140	0.0605	0.0005	0.0996	0.0014					612	8					
25.1	103	50	0.49	#####	0.45	5.659	0.085	0.0764	0.0012	0.1759	0.0027	1.762	0.060	0.0726	#####	1045	15	1031	22	1004	59	-4
26.1	69	24	0.34	-	0.52	9.407	0.374	0.0658	0.0019	0.1058	0.0042					648	25					
27.1	396	309	0.78	#####	2.67	14.800	0.520	0.0768	0.0017	0.0658	0.0023					411	14					
28.1	185	63	0.34	#####	0.01	5.352	0.082	0.0739	0.0009	0.1868	0.0028	1.901	0.040	0.0738	#####	1104	15	1081	14	1036	26	-7
29.1	674	401	0.59	#####	0.16	8.849	0.098	0.0641	0.0008	0.1128	0.0013					689	7					
30.1	708	81	0.11	#####	<0.01	9.036	0.108	0.0605	0.0005	0.1110	0.0013					678	8					
31.1	456	89	0.19	#####	0.06	9.547	0.139	0.0618	0.0010	0.1047	0.0015					642	9					
32.1	563	418	0.74	#####	0.03	9.812	0.127	0.0615	0.0005	0.1019	0.0013					625	8					
33.1	136	72	0.53	#####	0.39	5.582	0.102	0.0779	0.0008	0.1785	0.0033	1.836	0.046	0.0746	#####	1059	18	1059	17	1059	31	0
34.1	280	174	0.62	#####	0.11	6.046	0.236	0.0756	0.0012	0.1652	0.0064	1.702	0.075	0.0747	#####	986	36	1010	28	1061	32	7
35.1	344	128	0.37	#####	<0.01	9.326	0.120	0.0601	0.0012	0.1075	0.0014					658	8					
36.1	64	24	0.37	#####	0.28	6.035	0.109	0.0755	0.0015	0.1653	0.0030	1.666	0.054	0.0731	#####	986	17	996	21	1018	51	3
37.1	430	138	0.32	-	<0.01	10.162	0.126	0.0604	0.0006	0.0984	0.0012					605	7					
38.1	128	36	0.28	-	<0.01	5.950	0.097	0.0732	0.0010	0.1684	0.0027	1.738	0.041	0.0749	#####	1003	15	1023	15	1065	31	6
39.1	328	34	0.10	#####	0.04	6.148	0.089	0.0736	0.0006	0.1626	0.0024	1.642	0.029	0.0733	#####	971	13	987	11	1021	17	5
40.1	498	192	0.39	#####	0.09	5.841	0.080	0.0744	0.0006	0.1710	0.0023	1.736	0.030	0.0736	#####	1018	13	1022	11	1031	18	1
41.1	255	130	0.51	#####	0.36	6.420	0.101	0.0738	0.0007	0.1552	0.0024	1.516	0.034	0.0709	#####	930	14	937	14	953	28	2
42.1	13	3	0.19	#####	0.40	9.879	0.346	0.0640	0.0031	0.1008	0.0036					619	21					
43.1	314	99	0.31	#####	0.13	4.792	0.073	0.0829	0.0009	0.2084	0.0032	2.350	0.054	0.0818	#####	1221	17	1228	16	1240	30	2

- Notes:
1. Uncertainties given at the one σ level.
 2. f₂₀₆ % denotes the percentage of ²⁰⁶Pb that is common Pb.
 3. For areas >800 Ma, correction for common Pb made using the measured ²⁰⁴Pb/²⁰⁶Pb ratio.
 4. For areas <800 Ma, correction for common Pb made using the measured ²³⁸U/²⁰⁶Pb and ²⁰⁷Pb/²⁰⁶Pb ratios following Tera and Wasserburg (1972) as outlined in Compston *et al.* (1992).
 5. For % Conc., 100% denotes a concordant analysis.

spot number	spot age		$\delta^{18}\text{O}\text{‰}$	$\pm 1\sigma$	$^{176}\text{Hf}/^{177}\text{Hf}$	$\pm 2\sigma$	$^{176}\text{Lu}/^{177}\text{Hf}$	$\pm 2\sigma$	$\epsilon\text{Hf}(t)$	$\pm 2\sigma$	T_{DM} Ga
	Ma	\pm									
1	621	9	7.1537	0.181	0.282626	0.000025	0.001139	0.000051	7.77	0.89	0.99
2	609	8	8.4290	0.180	0.282428	0.000013	0.000563	0.000002	0.74	0.45	1.43
3	676	11	7.2280	0.178	0.282438	0.000015	0.000376	0.000003	2.68	0.52	1.36
5	1029	13	6.6960	0.181	0.282343	0.000017	0.000809	0.000032	6.87	0.59	1.37
6	1035	12	6.8572	0.179	0.282393	0.000027	0.000912	0.000026	8.72	0.96	1.26
7	664	10	8.7694	0.177	0.282406	0.000015	0.000329	0.000012	1.27	0.53	1.44
13	996	11	9.5896	0.179	0.282522	0.000047	0.001510	0.000065	12.00	1.66	1.02
15	1069	16	5.7397	0.177	0.282415	0.000015	0.000853	0.000008	10.29	0.52	1.18
21	1073	13	10.3911	0.179	0.282440	0.000037	0.001433	0.000025	10.85	1.31	1.15
24	612	8	10.7095	0.185	0.282761	0.000035	0.001937	0.000085	12.04	1.26	0.71
28	1104	15	6.0949	0.179	0.282308	0.000021	0.000484	0.000011	7.55	0.73	1.39
30	678	8	8.5188	0.179	0.282426	0.000018	0.000695	0.000034	2.12	0.62	1.40
32	625	8	6.5692	0.178	0.282474	0.000026	0.000724	0.000020	2.66	0.94	1.32
35	658	8	7.4773	0.184	0.282589	0.000028	0.001082	0.000057	7.30	0.98	1.05

Table 2. O- and Hf-isotope composition of zircon spots from sample TLT-2069

Age (Ma)	method	Lithology	Geological Unit	ϵ_{Hf}	ϵ_{Nd}	Hf T_{DM}	Nd T_{DM}	References
<i>Eastern Cordillera (NOA)</i>								
536 ± 5	1	Rhyolitic tuff	Puncoviscana Formation					Escayola et al. 2011
523 ± 5	1	Granodiorite	Cañani batholith					"
526 ± 13	1	Dacite	"					Hongn et al. 2010
534 ± 7	2	Gray granodiorite	"	+1.1 to -6.9	-5.1/-9.8	1.45	1.57/2.0	Hauser et al. 2011
541 ± 4	2	Red granitic facies	"		-5.0			"
523 ± 5	2	Porphyritic dacite	"	+0.4 to -3.8	-4.4 /-4.7	1.32/1.54	1.50	"
533 ± 2	2	Granite porphyry	Granite dykes					"
<i>Sierras Pampeanas of Córdoba and Guasayán</i>								
537 ± 4	1	Granodiorite (Hbl+Bt)	Sierra Norte-Ambargasta batholith		-5.8		1.69	Iannizzotto et al. 2013
537 #	3	I-type granitoids	"		-1.8/-5.4		1.39/1.66	"
530 ± 4	1	Granite	"		-5.5		1.67	"
535 ± 5	1	Metarhyolite	"					Von Gosen et al. 2014
534 ± 5	1	Granite porphyry	"					"
533 ± 4	1	Granite mylonite	"					"
531 ± 4	1	Dacitic phorphyry	"					"
530 ± 4	1	Granite	"					"
523 ± 5	1	Rhyolite to dacite	"					"
521 ± 4	1	Granite	"					"
519 ± 4	1	Rhyolite to dacite	"					"
533 ± 12	1	Porphyritic tonalite gneiss	"					Siegesmund et al. 2010
533 ± 2	1	Metaluminous O-gneiss	"		-5.8		1.7	Rapela et al. 1998
529 ± 2		Hb-Bt-Granodiorite	"		-4.3		1.6	"
532 ± 2	1	Dacite ??	"					Leal et al. 2003
512 ± 4	1	Dacite ????	"					"
515 ± 4	1	Granite	"					Stuart-Smith et al. 1999
540 #	3	I-type granitoids	"		-7.9		2.09	Escayola et al 2007
528 ± 2	1	Granodiorite	Sierra Norte-Ambargasta batholith? (Ascochinga unit)		-5.0		1.62	Rapela et al. 1998
527	1	Peraluminous granite	Pichanas					Lyons et al. 1997
ca. 548	1	S-type porphyritic granite	El Pílon granite complex					Stuart-Smith et al. 1999
523 ± 2	1	S-type granite	"		-5.6		1.69	Rapela et al. 1998
520 ± 3	1	Anatectic granite (U-Pb in Mo)	Suya Taco igneous complex					Tibaldi et al. 2008
529 ± 3.4	1	S-type granite	Juan XXIII pluton		-5.7		1.6/1.7	Escayola et al. 2007; Rapela et al. 1998
533 ± 4	2	Porphyritic granite	Guasayan pluton	-0.12 to -4.76		1.45 to 1.74		Dahlquist et al. 2016
<i>Saldania belt. Cape Granite Suite</i>								

510-523	1	A-type syenogranite	Darling batholith		+5.1	0.67	Chemale et al. 2011
524.2 ± 8.1	2	Syenite (A-type granite)	"		-3.66	0.76	"
547 ± 6	1	S-type granite	"		-3.5	1.56	da Silva et al. 2000
527.5 ± 8.2	2	Granite	George pluton		-5.8	1.71	Chemale et al. 2011
538.2 ± 1.9	2	Granodiorite	Peninsula batholith	-10.7/-2.3		1.39/1.71	Villaros et al. 2012
532.7 ± 1.9	2	Granite	"				"
536.2 ± 2.4	2	S-type microgranodioritic enclave	"	-6.3/+0.7		1.24/1.60	"
538.3 ± 1.5	2	Granodiorite	"	-1.5/+2.1		1.19/1.52	"
537.8 ± 1.6	2	S-type granite	"	-7.6/+1.2		1.10/2.16	Farina et al. 2014
536 ± 5	1	I-type granitoids	Robertson pluton		-3.1	1.63	da Silva et al. 2000
552 ± 4	1	S-type granite	Saldanha batholith				Scheepers and Armstrong 2002
540 ± 4	1	S-type granite	"				"
539 ± 4	1	S-type granite	"				"
515.5 ± 3	2	S-type ignimbrite	Postberg ignimbrite				Scheepers and Pujol 2002

Saldania belt. Cape Granite Suite (cont.)

Estimated age					ϵNd	$\text{Nd } T_{\text{DM}}$	
550-530	3	Granites	Maalgaten granite		-4.47	1.88	Chemale et al. 2011
550-531	3	"	Olifantskop granite		-3.29	1.72	"
550-532	3	"	Darling batholith		-4.25	1.54	"
550-533	3	"	Woodville granite		-4.94	1.60	"
550-534	3	"	Rooiklip granite		-5.85	1.71	"
540	3	"	Riviera pluton		-2.1	1.01	"
540	3	"	Haelkraal granite		-2.78	1.99	"
540	3	"	Paarl pluton		-1.87	1.23	"
540	3	"	Paarl pluton		-1.92	1.89	"
540	3	"	Greyton granite		-3.63	1.49	"
540	3	"	Robertson pluton		-3.08	1.41	"
540	3	"	Schapenberg granite		-1.44	1.32	"
540	3	"	Swellendam granite		-3.89	1.45	"
540	3	"	Worcester mylonite		-1.78	1.21	"
540	3	"	Cape Columbine granite		-2.56	1.39	"

Table 3. Compilation of ages of Pampean-Saldanian igneous rocks and of isotope data (Nd and Hf in zircons)

Region and lithology	Metamorphic event	Mineral assemblage	<i>P-T</i> conditions	References
<i>Low- to mid-temperature domain</i>				
Puncoviscana Formation NW Argentina	M ₁ (HP/LT)	Wm+Chl+Qz	<i>b</i> parameter of 9.035-9.055 Å (intermediate-high pressure) CIS 0.23-0.36 °Δ2θ (anquizone-epizone) 240-300 °C, 8-9 kbar (1)	Do Campo y Nieto (2003) y Do Campo et al (2013)
	M ₂ (LP/LT)	Wm+Chl+Qz	275-350 °C, 0.7-3 kbar (1)	
<i>High-temperature domain (Sierras de Córdoba)</i>				
Cordierite diatexite (El Pilón)	M ₂ (MP/HT)	Grt (core)+Pl (core)+Crd1 (matrix)+Sil+Qz	780 °C, 5.9 kbar (1)	Rapela et al. (2002)
Restite in monzogranite (el Pilón)	M ₃ (LP/MT-HT)	Crd+Bt+Ms+Sil+Qz+Pl±K fs	550 ±50 °C, 3.3 ± 0.6 kbar (1)	
Garnet-cordierite diatexite. Central Sierra Chica	M ₂ (MP/HT)	Grt+Sil+Crd+Qz+Bt+Kfs	820±25 °C, 5.7±0.4 kbar (1)	Baldo et al. (1996) and Rapela et al (1998)
	M ₃ (LP/MT-HT)	Sp+Sil+Crd+Kfs	715±15 °C, 4±0.5 kbar (1)	
Garnet-biotite gneis. Central Sierra Chica	M ₂ (MP/HT)	Grt+Kfs+Qz+Pl+Sil+Bt and relictic Ky	820±60 °C, 6.3±1 kbar (1)	
Banded garnet gneisses. Southern Sierra Chica	M ₂ (MP/HT)	Grt (core)+Bt+Pl+Sil+Qz	715-814 °C, 7.3-8.6 kbar (2)	
	M ₃ (LP/MT-HT)	Grt (rim)+Bt+Pl+Sil+Qz	598-710 °C, 5.2-7.2 kbar (2)	
Garnet-biotite gneisses. Northern Sierra de Comechingones	M ₂ (MP/HT)	Grt+Bt+Qz+Pl+Rt	760±30 °C, 3±0.5 kbar (3)	Otamendi et al. (1999)
	M ₃ (LP/MT-HT)		600 °C, 5.8 kbar (3)	
Garnet±cordierite migmatites. Northern Sierra de Comechingones	M ₂ (MP/HT)	Grt+Bt+Qz+Pl+Sil+Rt+Ilm	800-900 °C, 7-8.3 kbar (3)	
	M ₃ (LP/MT-HT)	Grt+Bt+Qz+Pl+Sil	700-750 °C, 6.5-6.9 kbar (3)	

Garnet-orthopyroxene granulite. Northern Sierra de Comechingones	M ₂ (MP/HT)	Grt+Opx+Pl+Qz	850±50 °C, 7.1-8.5 kbar (3)	Otamendi et al. (2005)
Garnet-cordierite granulite. Northern Sierra de Comechingones	M ₂ (MP/HT)	Grt+Crd+Pl+Sil+Qz	790 °C, 8±0.5 kbar (3)	Otamendi et al. (1999)

Table 4. Summary of representatively thermobarometry data from low- to mid-temperature and high-temperature domains. (1) TWQ method (Berman, 1991). (2) Thermometer GB (garnet-biotite; Holdaway et al., 1997) and barometer GASP (garnet, sillimanite, quartz and plagioclase; Koziol, 1989). (3) Conventional thermometry (multi-equilibrium).

parameter	S. Pampeanas + NOA		Saldanian Belt	
	S-type	I-type	S-type	I-type
Age (Ma)	529 ± 3 to 520 ± 3 ca. 523	541 ± 4 to 523 ± 5 ca. 530	552 ± 4 to 533 ± 2 ca. 540 527 ± 8 (late)	536 ± 5
A/CNK	1.1 - 1.4	0.95 - 1.03	1.0 - 1.7	0.9 - 1.1
eNd	-5 / -6	-4 / -10	-3 / -5	-1.4 / -3.9
TDM (Ga)	1.6 - 1.7	1.5 - 2.0	1.5 - 1.9	1.0 - 2.0
eHf		+1.1 / -6.9	-11 / -0.2	
TDM (Ga)		1.3 - 1.7	1.1 - 2.0	

Table 5. Summary of age and geochemical characteristics of igneous rocks from the Pampean and the Saldanian belts

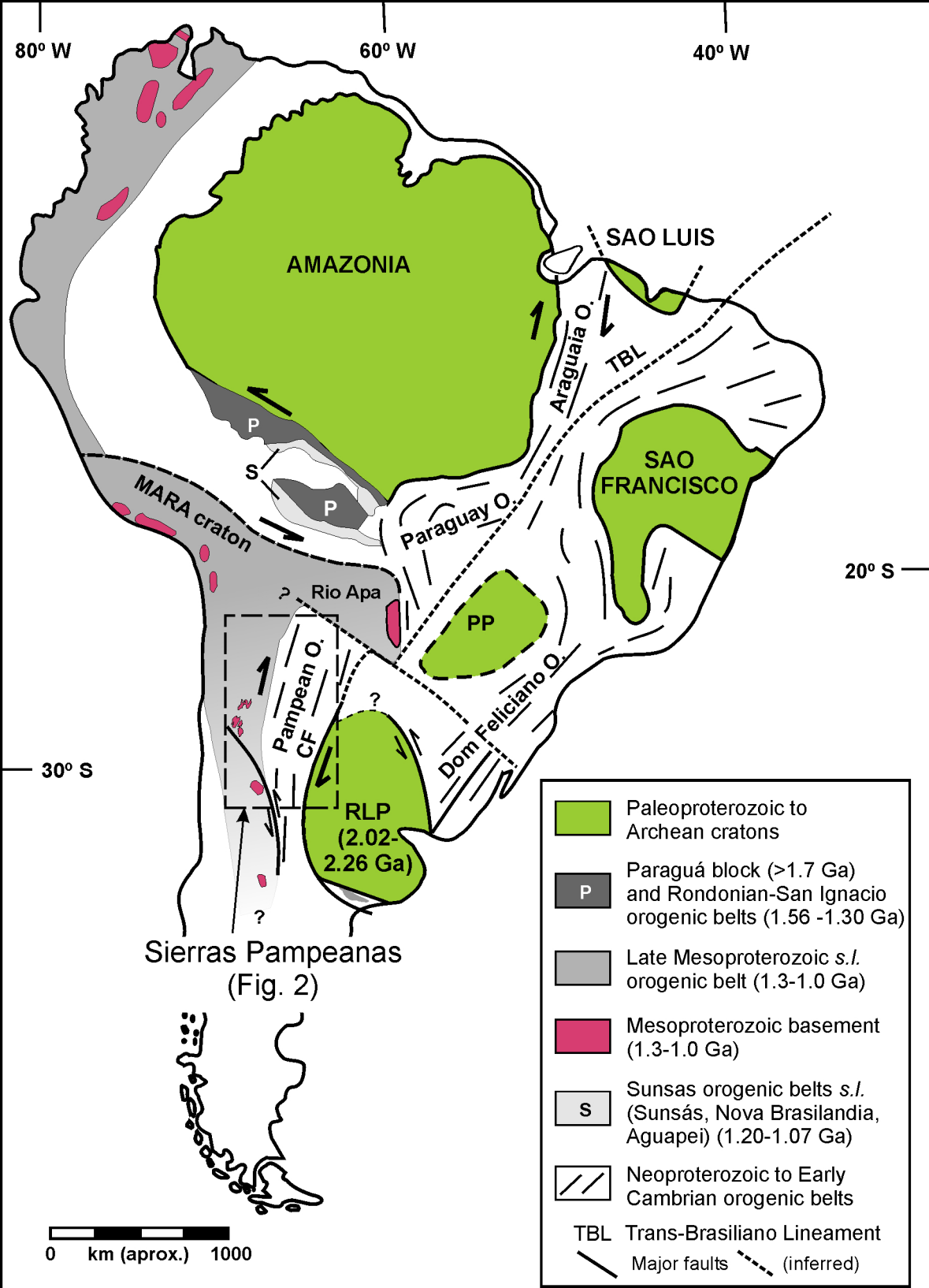


Figure 1

LEGEND

METASEDIMENTARY ROCKS

Post-Pampean Cambrian sedimentary rocks



Pre-Pampean

Puncoviscana F. (low grade)



Undifferentiated Puncoviscana Fm. and Ediacaran to early Cambrian cover (MARA) (high grade)



Grenville-age basement and Ediacaran to early Paleozoic cover (MARA)



IGNEOUS ROCKS

Devonian Granites



Famatinian (Ordovician)



Cambrian (Pampean)



TECTONICS

Pampean orogen



Pampean orogen reworked by the Famatinian orogeny (low- to high-grade metamorphism)



Pampean suture ?

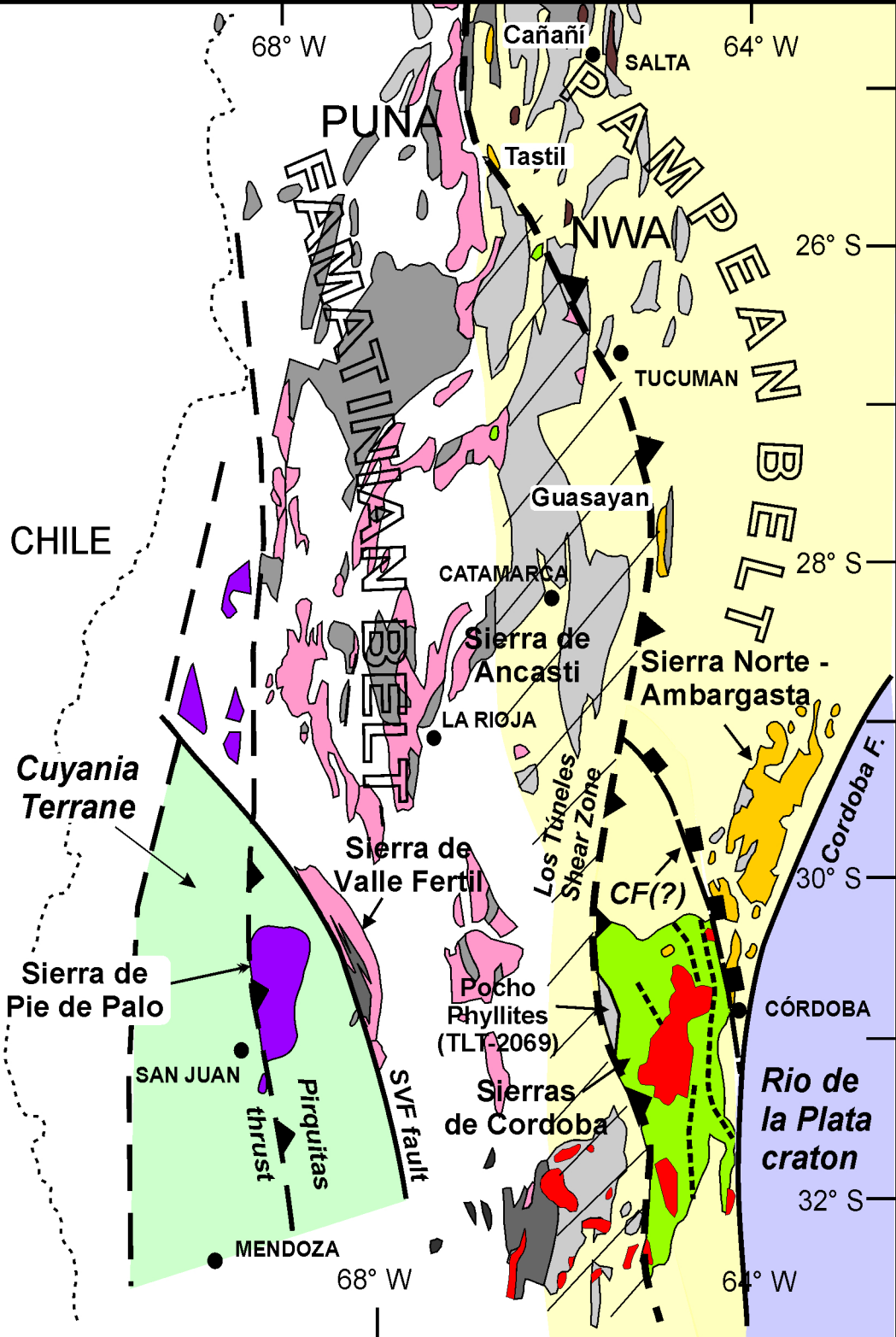
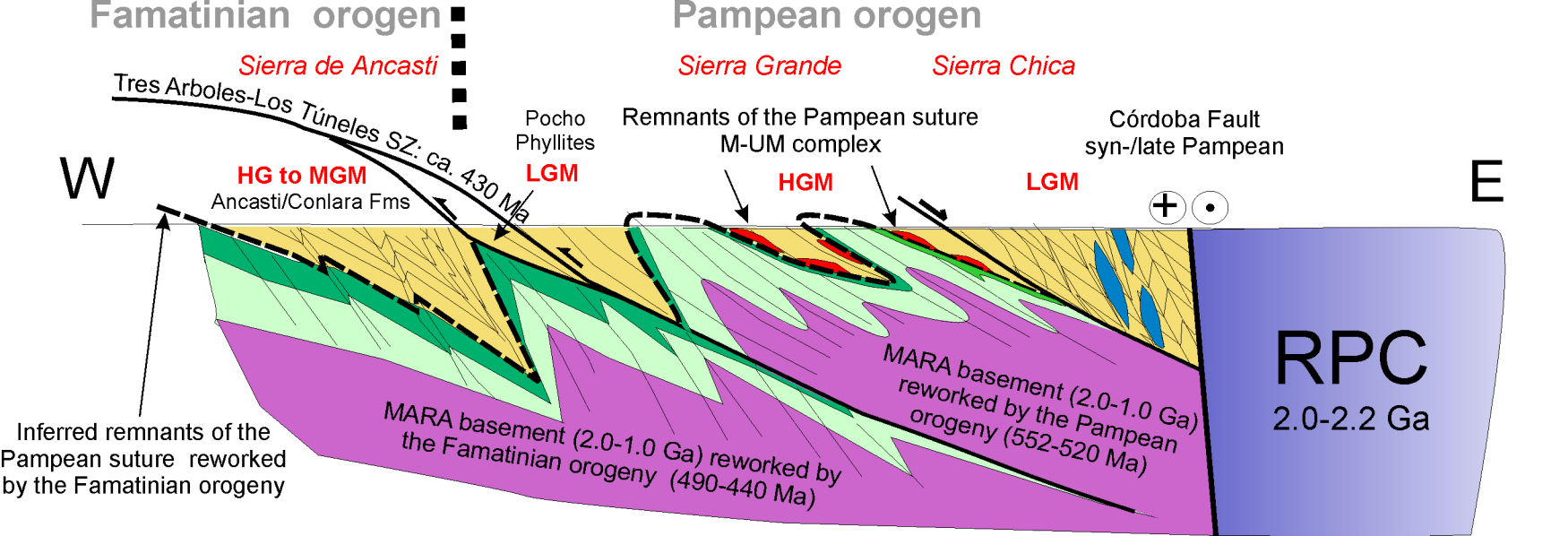




Fig. 2

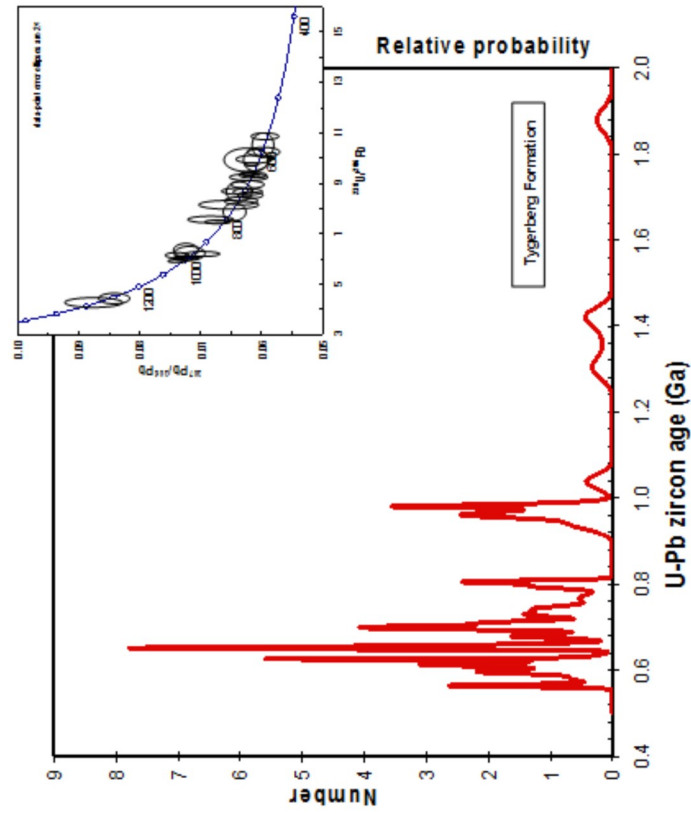
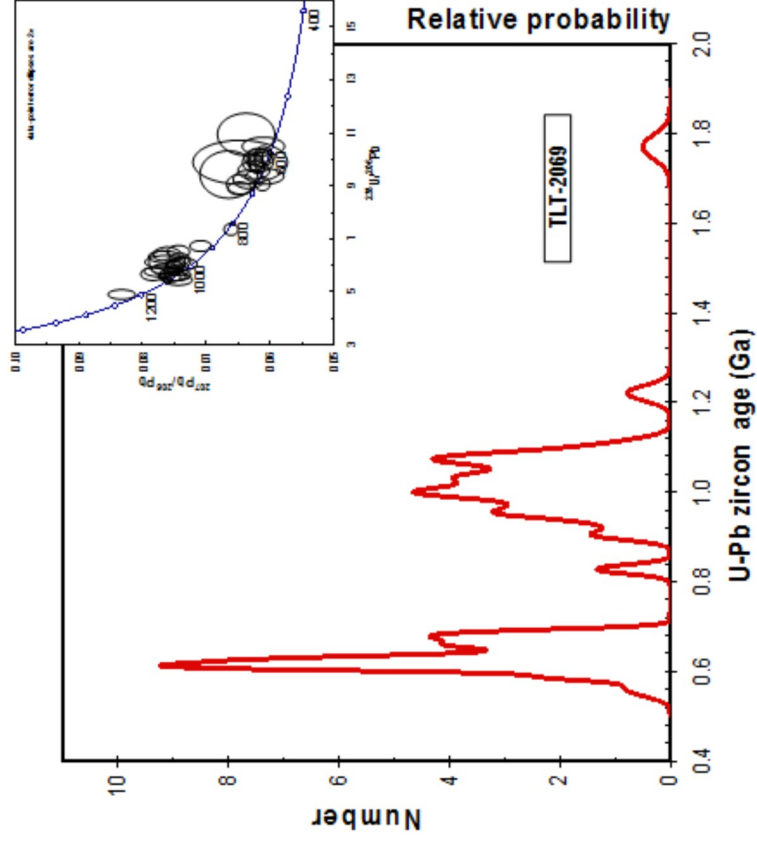


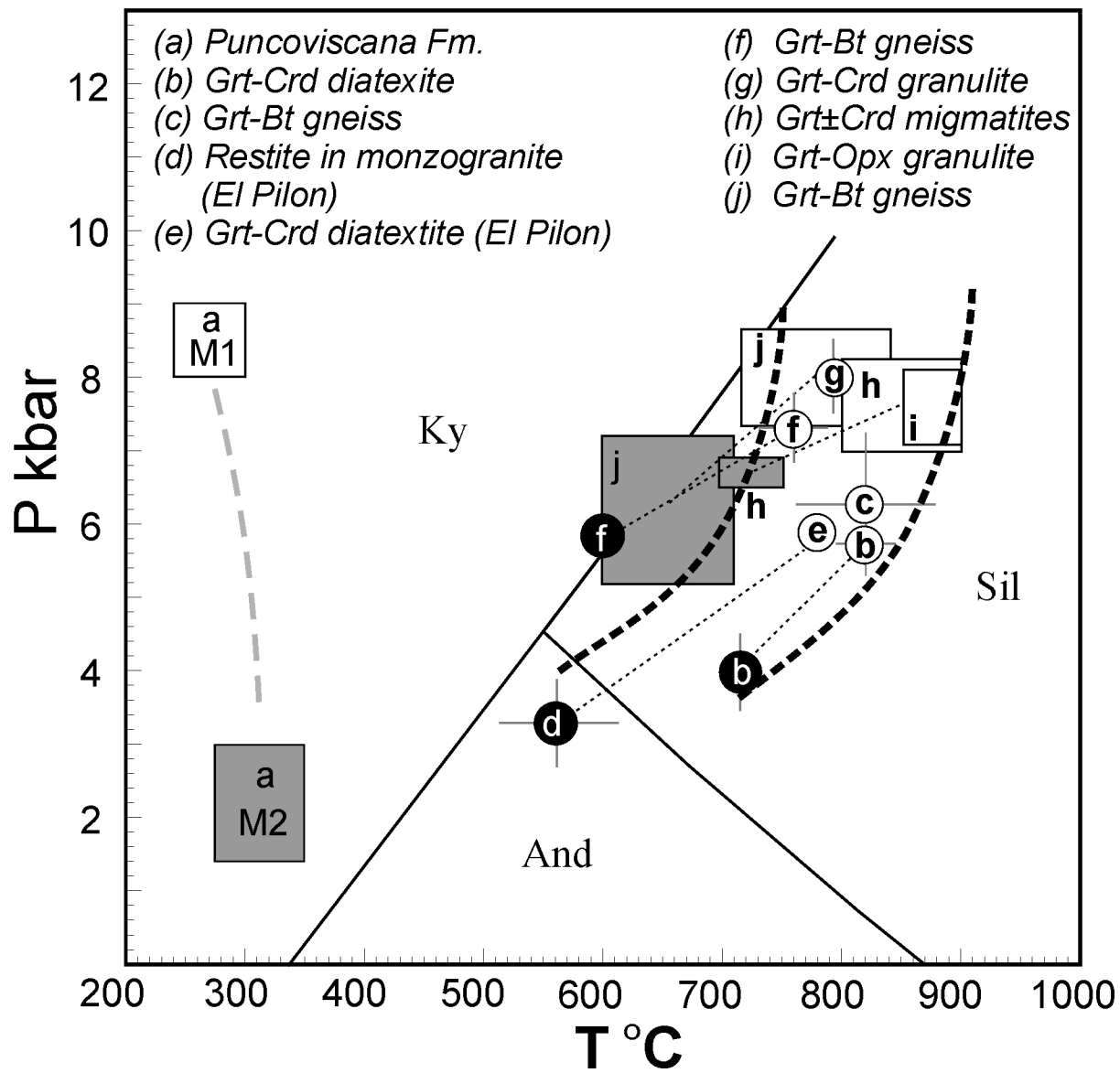
 Meta-greywacke, schists & gneisses (Puncoviscana Formation) (570-530Ma)

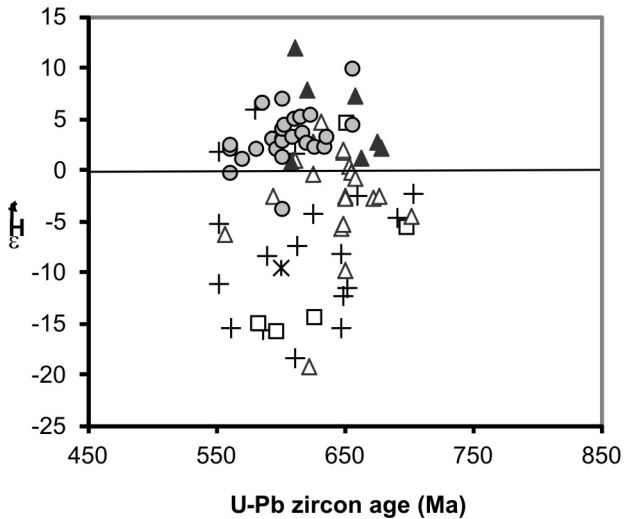
 Marbles, calc-silicate rocks (Ediacaran to early Cambrian)

 Quartzites, schists & gneisses with WSP-type detrital zircon age patterns

 Mafic-Ultramafic igneous complex (inferred Pampean ophiolite)  Pampean I-type magmatic arc (545-530 Ma)

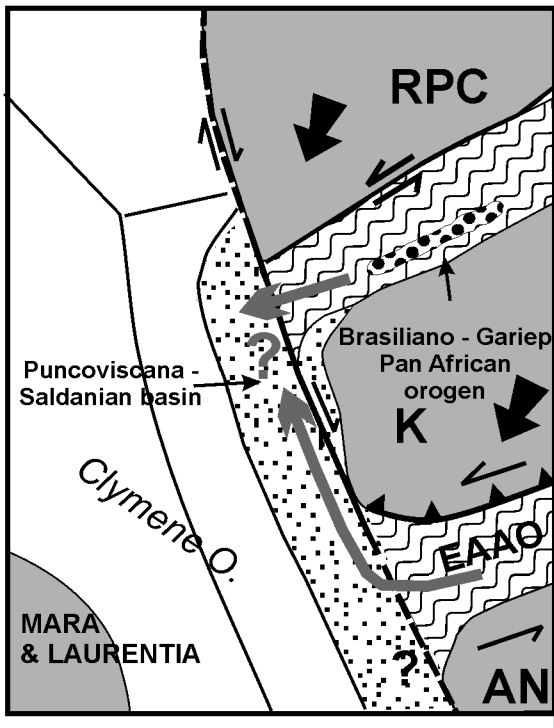




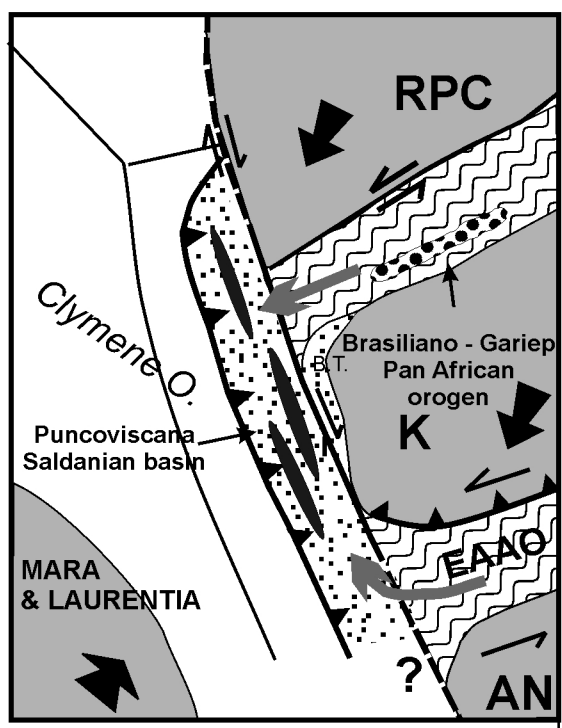


- + Puncoviscana
- Tygerberg Form.
- △ Swartland
- * Boland
- ▲ TLT-2069
- Mecubúri Group

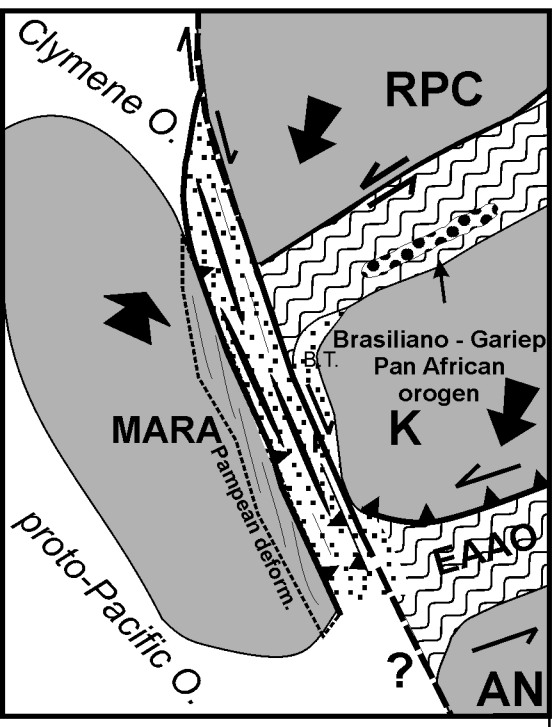
(b) 570 - 552 Ma



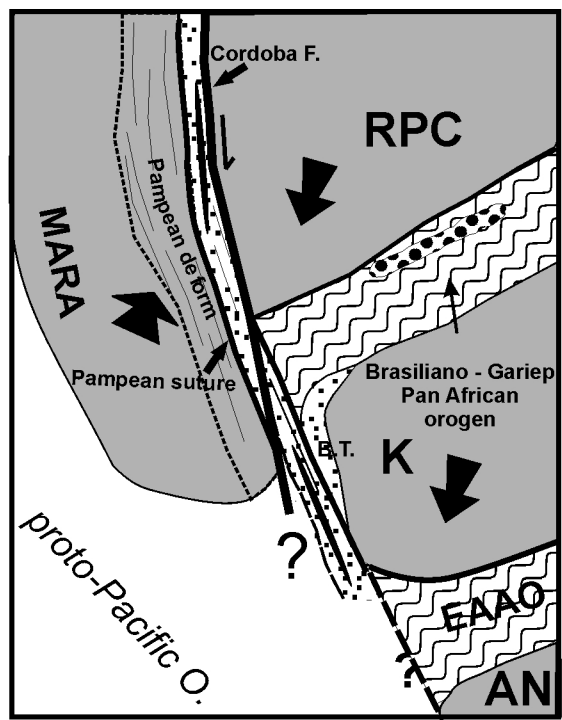
(b) 552 - 530 Ma



(b) 530 - 520 Ma



(b) <520 Ma



Legend for Figure 7:

- Cratons (Solid grey)
- Sedimentary Basins (Dotted pattern)
- Collisional orogenic belts (Wavy lines)
- Magmatic arcs (Diagonal lines)
- Direction of palaeoflow (Arrow)

Figure 7